HHS Public Access

Author manuscript

Sci Transl Med. Author manuscript; available in PMC 2018 March 12.

Published in final edited form as:

Sci Transl Med. 2017 July 12; 9(398): . doi:10.1126/scitranslmed.aal1243.

Zbtb7a induction in alveolar macrophages is obligatory in anti-human leukocyte antigen-mediated lung allograft rejection

Deepak K. Nayak[1], **Fangyu Zhou**[2], **Min Xu**[2], **Jing Huang**[3], **Moriya Tsuji**[3], **Jinsheng Yu**[4], **Ramsey Hachem**[5], **Andrew E. Gelman**[2], **Ross M. Bremner**[1], **Michael A. Smith**[1], and **Thalachallour Mohanakumar**[1,*]

[1]Norton Thoracic Institute, St. Joseph's Hospital and Medical Center, Phoenix, AZ.

[2]Department of Surgery, Washington University School of Medicine, St. Louis, MO.

[3]HIV and Malaria Vaccine Program, Aaron Diamond AIDS Research Center, Affiliate of the Rockefeller University, New York, NY.

[4]Genome Technology Access Center, Department of Genetics, Washington University School of Medicine, St. Louis, MO.

[5]Department of Medicine, Washington University School of Medicine, St. Louis, MO.

Abstract

Chronic rejection (CR) significantly limits long-term success of solid organ transplantation. *De novo* antibodies to mismatched donor human leukocyte antigen (DSA) following human lung transplantation (LTx) predispose lung grafts to CR. We sought to delineate mechanisms and mediators of DSA pathogenesis, and to define early inflammatory events that trigger CR in LTx recipients and obliterative airway disease (a correlate of human CR) in a murine model. Induction of transcription factor Zn finger BTB domain containing protein 7A (Zbtb7a) was an early response critical in DSA-induced CR. A cohort of human LTx recipients that developed DSA and CR demonstrated greater Zbtb7a expression long before clinical diagnosis of CR compared to non-rejecting LTx recipients with stable pulmonary function. Expression of DSA-induced Zbtb7a was restricted to alveolar macrophage (AM), and selective disruption of Zbtb7a in AM resulted in less bronchiolar occlusion, low immune responses to lung-restricted self-antigens, and high protection from CR. Additionally, in allogeneic cell transfer protocol, antigen presentation by AM was Zbtb7a-dependent, whereas AMs deficient in Zbtb7a failed to induce antibody and T cell responses. Collectively, we demonstrate that AM plays an essential role in antibody-induced pathogenesis of CR by regulating early inflammation and lung-restricted humoral and cellular

*To whom correspondence should be addressed: Tm.Kumar@dignityhealth.org.

Author contributions: DKN and TM conceived the idea and designed the research studies; DKN and FZ conducted the experiments; JH and MT developed/provided reagents used in the study; MX assisted with immunofluorescence studies; JY evaluated the microarray data; RH assisted with patient selection and clinical sample procurement; DKN, FZ, RH and TM evaluated clinical history of LTx recipients; DKN, FZ and TM analyzed the data; DKN and TM wrote the manuscript; JH, MT, AEG, RMB, MAS and TM critically reviewed the manuscript.

Competing interests: Authors have no competing financial interests to disclose.

Data and materials availability: Microarray Data are available at NCBI GEO database (GEO ID: GSE71426, https://www.ncbi.nlm.nih.gov/geo/query/acc.cgi?token=wvuhuuuwnzafnst&acc=GSE71426).

autoimmunity. The AM-centric responses were Zbtb7a-dependent, whereas Zbtb7a-sufficient AM (not Zbtb7a-deficient AM) initiated and/or amplified DSA and DSA-induced effector functions.

Introduction

Elicitation of immune responses to mismatched donor human leukocyte antigen (HLA) and breakdown of tolerance to self-antigen (SAg) pose significant challenges to the initial graft acceptance and its continued function after solid organ transplantation (1, 2). Lung transplantation (LTx) is a viable lifesaving intervention in many end-stage respiratory diseases such as chronic obstructive pulmonary disease, cystic fibrosis, idiopathic pulmonary fibrosis, alpha-1 antitrypsin deficiency, pulmonary arterial hypertension, interstitial lung disease, and bronchiectasis; however, its success is limited: more than 50% of recipients develop chronic rejection (CR), clinically diagnosed as bronchiolitis obliterans syndrome (BOS) within five years of transplantation (3, 4). BOS is a state of irreversible loss of respiratory function that does not normally respond to immunosuppressive regimens. Although the etiology of BOS is unclear and the mechanisms of lung allograft rejection are poorly defined, *de novo* antibody (Ab) to mismatched donor HLA (DSA), even when non-persistent, is a significant risk factor for CR (5–9). The immunodominant role of DSA in CR pathogenesis is supported by three distinct observations: 1) *de novo* DSA is associated with recurrent and high-grade cellular rejection and lymphocytic bronchiolitis (7, 10, 11) and an early *de novo* DSA is a significant risk factor for CR (12); 2) DSA development often precedes *de novo* Ab and T cell responses to lung-restricted SAgs (Collagen V [Col V] and K-alpha 1 Tubulin [Kα1T]) (8); and 3) DSA depletion via Ab-directed therapies lowers BOS hazard ratio and improves freedom from BOS (5, 13–15).

In addition to the elicitation of DSA and consequent immune responses to lung-restricted SAgs, preexisting anti-Col V and anti-Kα1T in prospective LTx recipient (LTxR) pre-transplantation significantly correlate with increases in primary graft dysfunction, *de novo* DSA, and BOS (16, 17). In a preclinical mouse model of obliterative airway disease (OAD), exogenous anti-major histocompatibility complex (MHC) delivered to native lungs recapitulated many histopathological correlates of BOS and elicited Col V and Kα1T specific immune responses (18, 19). The proximal mechanisms and effectors of immune activation for anti-MHC are unknown and must be defined to facilitate early detection and possible intervention in Ab-induced lung inflammation. We hypothesize that Ab ligation of MHC elicits a set of “early triggers,” culminating in activation of immune responses to lung-restricted SAgs and leading to epithelial metaplasia, airway fibrosis, and airway occlusion—cardinal signs of CR.

Alveolar macrophage (AM), an embryonic phagocyte derived from erythro-myeloid progenitor (20–23), is a luminal sentinel for pulmonary pathogens and pollutants (24, 25). AMs represent the vast majority (>80%) of the lung-resident macrophages, occurring at a density of up to 12 cells per alveolus (26, 27), are essential in the functional preservation of respiratory epithelium (25, 28), containment of airway infection and inflammation (29–32), and elicitation of intranasal vaccine-induced immunity (33, 34). AMs bear functional significance from the LTx perspective as mature lungs contain high load of AM (up to 6×10^9

in humans and up to 3×10^6 in mice) (26); allogeneic AMs in a rodent LTx model play a major role in lung allograft rejection by shaping T and B cell repertoires (35). Our analysis of the extractable cells in bronchoalveolar lavage (36), supported by evaluation of lung tissue biopsies (37) from LTxRs, revealed long-term sustenance (up to 3.5 years) of donor-derived AMs in the transplanted lungs. Besides serving as a reservoir for donor antigen(s), donor AMs were capable of inducing DSA and responded to DSA with production of pro-inflammatory cytokines (36). Adoptive transfer of single antigen mismatched AM bearing a macrophage-specific MHC class I transgene induced *de novo* DSA, Col V- and Kα1T-directed T cell and B cell autoimmunity, and OAD. This functional duality in which AM can initiate genesis and influence pathogenesis of DSA indicated an important role for AMs in Ab-mediated lung graft rejection. In this communication, we describe induction of a transcription factor, zinc finger and BTB domain containing 7a (Zbtb7a), in AM as an indicator and a critical regulator of the anti-MHC induced inflammation and OAD.

Zbtb7a, initially discovered as a proto-oncogene (38), regulates development and function of lymphocytes and tissue-resident macrophages (39), and its global deficiency triggers embryonic lethality by impairing erythropoiesis (40). Zbtb7a is essential for B cell neogenesis (41), mature B cell function (42), CD4 differentiation (43), and preservation of peripheral T helper (Th)1 and Th17 phenotypes (44, 45). It also regulates bone resorption by osteoclasts (46, 47). Functional pleiotropy of Zbtb7a further involves T cell repertoire purging by regulating intrathymic antigen expression (48), oncosuppression in prostate cancer (49), and repression of fetal hemoglobin synthesis in adults (50). Given the participation of Zbtb7a in oncogenesis, hematopoiesis and immunity, its involvement in pulmonary inflammation and autoimmunity is unknown. The chronic inflammation in BOS is a condition of fibroproliferation with involvement of autoimmune components that often leads to pulmonary lymphoid neogenesis (51). In this study, we identified Zbtb7a as an early molecular signature and have established its dominant role in the initiation and amplification of Ab-induced inflammatory circuits in the cellular and humoral autoimmunity associated with chronic lung graft rejection.

Results

A unique lung transcriptional landscape induced by Ab ligation of MHC class I

Global changes in the gene expression of C57BL/6 lungs treated with anti-H-$2K^b$ were compared with those of the immunoglobulin G isotype control after 4 h on one, two, three and six days post-Ab administration. A differential expression was observed, with 14 genes significantly upregulated (>1.5 fold, Log2; $p<0.05$ and FDR q<0.1) after MHC class I ligation compared to the isotype control (Fig. 1A). Most significant was the upregulation of transcription factor Zbtb7a (1.68862 fold, $p=1.08E^{-05}$) also known as Pokemon or leukemia/lymphoma-related factor (38, 52) (Fig. 1B, sTable1). Induction of Zbtb7a was detected in lungs on day 2 after anti-H-$2K^b$ administration; its expression increased further at subsequent time points (Fig. 1C). Concurrently, 97 genes were significantly down-modulated in the anti-H-$2K^b$-administered lungs ($p<0.05$). Based on established functions of Zbtb7a, we reasoned that Zbtb7a exerts a major effect on the early events that lead to development of immune responses to lung-restricted SAgs and OAD.

In addition to transcript analyses, we evaluated influence of anti-MHC class I ligation on preponderance of lung-infiltrating leukocytes (sFig. 1). Anti-H-2K^b resulted in a massive neutrophil influx as early as 4 h post-Ab administration and led to a persistent neutrophilia. Accumulation of lung-trophic B cells also occurred, *albeit* at a slower pace (increase in B cell numbers was significant on day 6; $p<0.05$). Th cell (CD4+), T cytotoxic cell (CD8+), and AM compartments, however, remained unchanged.

Reduced accumulation of lung-trophic leukocytes and formation of inducible bronchus-associated lymphoid tissue in Zbtb7a-deficient lungs

A targeted disruption of Zbtb7a gene function was performed by si-RNA via a lentiviral delivery system (Fig. 2A). *In vivo* lentivirus gene delivery is effective in specific targeting and long-term transformation of AMs (53, 54). In the present study, si-Zbtb7a lentivirus reduced lung Zbtb7a expression approximately by 15 fold, compared with expression in the si-scrambled control (Fig. 2B). Expression of Zbtb7a remained consistently low in the si-Zbtb7a transduced lungs for about 5 months (*i.e.*until the conclusion of analysis), indicating persistent repression of the target gene expression. Furthermore, induction of Zbtb7a at protein level occurred in anti-H-2K^b administered si-scramble transduced lungs, but not in si-Zbtb7a transduced lungs (Fig. 2C).

The early influx of inflammatory cells induced by anti-MHC (sFig. 1) prompted us to evaluate the composition of lung-infiltrating leukocytes after Zbtb7a knockdown. Though B cells and neutrophils were the predominant cell types in Zbtb7a-sufficient (si-Scramble transduced) lungs, the Zbtb7a-deficiency (si-Zbtb7a transduced lungs) resulted in an 83% reduction in total neutrophils (sFig. 2). The Zbtb7a-deficient lungs also demonstrated a 59% decrease in total B cells compared to that in Zbtb7a-sufficient lungs. Deficiency of Zbtb7a, however, did not alter the T cell (CD4+ and CD8+) and AM compartments in response to anti-MHC ligation, which remained unchanged between the treatment groups. These results suggested a proinflammatory role for Zbtb7a in Ab-induced lung inflammation.

Ectopic formation of inducible bronchus-associated lymphoid tissue (iBALT) is known to function as a local depot for immunologic priming and activation, and is induced in native as well as transplanted lungs as a response to Abs, infection, inflammation, and graft rejection (55–58). Our results demonstrate a marked reduction in the frequency of iBALT formation in anti-H-2K^b administered mice (>175% for percent-iBALT-positive and >600% for iBALT per level) following Zbtb7a depletion (*i.e.*si-Zbtb7a) compared to si-scramble with intact Zbtb7a expression (sFig. 3).

Induction OAD and immune responses to lung-restricted SAgs in Zbtb7a-sufficient lungs, but not in Zbtb7a-deficient lungs, as a response to anti-MHC class I

Induction of OAD was done according to our previously described protocol (18), with repeated intrabronchial administration of anti-H-2K^b (Fig. 2A). At 45 days post-Ab administration, lung Zbtb7a expression and histopathology were assessed, and immune responses to lung-restricted SAgs were measured. Anti-H-2K^b administration in scrambled si-RNA-treated mice led to bronchiolar hypertrophy, mononuclear leukocytic infiltrations and intraluminal as well as peribronchiolar fibrosis with near-complete obliteration of the

small airways (Fig. 2D–E). The Zbtb7a-deficient mice, on the other hand, showed a marked reduction in the OAD pathology, with preservation of near-normal bronchiolar architecture and minimal collagen deposition (Fig. 2D–E).

Development of *de novo* Abs to Col V and Kα1T is a measure of autoimmunity following human LTx (8, 16) and in animal models of CR (18, 19). Zbtb7a deficiency resulted in a marked decline in anti-MHC-induced OAD concomitant with a steady rise in the serum anti-Col V and anti-Kα1T titers that occurred in Zbtb7a-sufficient mice (si-scramble) reaching >650 μg/mL at day 45 (Fig. 2F). Remarkably, Zbtb7a-deficient mice failed to induce Abs to Col V and Kα1T. Further, elicitation of Col V- and Kα1T-specific IFN-γ and IL-17 producing T cells was significantly lower in si-Zbtb7a transduced lungs than in si-scramble, indicating a Zbtb7a-dependent impairment of the cellular immune activation (Fig. 2G). Although there was no change in the number of IL-4-producing cells between treatment groups, marginal increases in Col V- and Kα1T-specific IL-10-producing cells were observed in Zbtb7a knockdown mice (58% and 65% increases, respectively; Fig. 2G).

Upregulation of ZBTB7A in human LTx recipients with de novo DSA and BOS

In order to evaluate the clinical relevance of ZBTB7A as a measure of response(s) to *de novo* DSA, we analyzed BAL specimens from 139 LTxRs (sTable 2). ZBTB7A expression at three months post-LTx was the designated baseline level. Cohorts of LTxRs were constituted with LTxs performed at similar time frame and receiving similar immunosuppression. We compared 21 LTxRs who developed DSA and were diagnosed with BOS against 21 LTxRs with no detectable DSA with stable pulmonary function. We found a significantly higher ZBTB7A expression in patients with BOS at the time of diagnosis compared to that of stable patients (2.44 fold vs 1.02 fold, respectively; Fig. 3A). Furthermore, kinetics of ZBTB7A expression were evaluated at six and 12 months post-LTx in 12 LTxRs who later developed BOS (onset between 36 and 59 months post-LTx) and in 11 BOS-free LTxRs with stable pulmonary function up to 65 months post-LTx (Fig. 3B–C). In this cohort, nine LTxRs who developed BOS had documented *de novo* DSA to mismatched donor HLA, whereas BOS-free LTxRs did not have DSA. An elevated ZBTB7A (2.9 fold) was evident at six months; this increased to 5.6 fold at 12 months in BOS patients where as the corresponding increase varied between 1.1 fold and 1.2 fold in stable patients.

Elicitation of *de novo* DSA is an independent and significant risk factor for development of BOS after human LTx (16). The kinetics of ZBTB7A induction followed the trend of DSA in which high ZBTB7A expression coincided with the peak DSA level, after which it progressively declined with reduction in DSA (Fig. 3D). This cohort of LTxRs developed DSA at 7±3 months post-LTx and was treated with Ab-directed therapies (*i.e.*rituximab and intravenous immunoglobulin). In LTxRs who did not develop DSA and were stable without evidence of rejection, however, there was no significant induction of ZBTB7A up to 2 years post-LTx (Fig. 3E). Because DSA and Abs to lung-restricted SAgs are predisposing factors for BOS, we differentially assessed the association of DSA and Abs to lung-restricted SAgs with ZBTB7A expression. LTxRs who developed DSA stimulated significantly higher ZBTB7A expression than LTxRs who did not develop DSA (Fig. 3F). In the DSA^{-} group (at

time of analysis), those who developed Abs to lung-restricted SAgs elicited greater ZBTB7A expression compared to LTxRs who did not develop these autoimmune responses. Moreover, DSA^+ LTxRs who developed Abs to SAgs registered a far greater ZBTB7A induction than recipients who developed DSA alone (*i.e.*without Abs to lung-restricted SAgs), suggesting a synergetic effect. It is of interest that peripheral blood leucocytes collected from LTxRs at the time of BAL collection revealed no significant changes in ZBTB7A expression (irrespective of BOS or DSA outcomes; data not shown). This suggests that ZBTB7A induction may be a local phenomenon. Collectively, these results demonstrate a positive association between dynamics of post-LTx *de novo* DSA and BAL cell ZBTB7A expression.

Localization of anti-MHC induced Zbtb7a expression to AMs

To ascertain the cellular origin of Zbtb7a expression in the lungs, we fractionated BAL leukocytes into Siglec-F^+ and $CD11c^+$ (AM) and Siglec-F^- and $CD11c^-$ (non-AM) and isolated respiratory epithelial cells. Lentiviral delivery of si-RNAs did not induce Zbtb7a expression, *per se* (Fig. 4A). Transcript for Zbtb7a was detectable only in the AM fraction from si-scramble lungs following anti-MHC administration. Furthermore, no expression of Zbtb7a was detected in non-AM BAL cells or in alveolar epithelial cells. In contrast, anti-MHC failed to mount Zbtb7a induction in si-Zbtb7a transduced lungs. These results indicate that the predominant Zbtb7a signal following MHC ligation was localized *in vivo* to AMs. Furthermore, AMs with induced Zbtb7a also expressed chemokine (C-X-C motif) ligand [(Cxcl)] 13 and Cxcl15 involved respectively in B cell and neutrophil chemotaxis (59, 60), and matrix metallopeptidase (Mmp) 9, a type IV collagenase involved in remodeling of extracellular matrix (ECM) (61).

To validate the *in vivo* findings and delineate sufficiency of MHC ligation in Zbtb7a induction, purified AMs were analyzed in an *in vitro* culture system. Stimulation by anti-HLA ABC (W6/32), but not isotype-matched control (C1.18.4), elicited ZBTB7A expression in human AMs (Fig. 4B). However, such an induction was not evident in non-AM BAL cells that mostly consisted of lymphocytes and granulocytes. In parallel, mouse AMs were evaluated for their responses to MHC class I (AF6-88.5.5.3) and class II (M5/114) ligations. Both of the MHC stimuli resulted in a significantly higher Zbtb7a expression in murine AMs compared to respective isotype controls (Fig. 4B).

Further analysis of the fractionated AM and non-AM BAL cells and lung-tissue collected by needle biopsies revealed higher induction of ZBTB7A in AMs. Purified AMs from BOS patients recorded a >5 fold higher ZBTB7A expression over the non-AM BAL cells and biopsies from the same patient collected on the same day (Fig. 4C). Moreover, none of the AM, non-AM, or biopsy specimens from BOS-free LTxRs with stable pulmonary function induced ZBTB7A expression. Demonstration of the localized induction of ZBTB7A in AMs from BOS patients further signifies an important role for AM in clinical disease development (Fig. 3A–C).

Induction of Zbtb7a and OAD following Ab ligation of AM MHC class I

We utilized a novel C57BL/6-based transgenic (Tg) mouse model, huCD68-K^d Tg C57BL/6, which expresses full-length H-$2K^d$ transgene in C57BL/6 (H-$2K^b$) macrophages (62) to delineate the specific role(s) of AM in anti-MHC pathogenesis. The BAL cells from naïve lungs were predominantly (>80%) AM that concurrently expressed H-$2K^d$ and H-$2K^b$ on cell surface (Fig. 5A). Additionally, expression of $CD11b^{low}$ and $F4/80^{int}$ in Tg AMs was comparable with their wild-type counterparts (C57BL/6 AMs) and was consistent with the AM lineage markers (25, 28). Following a lentivirus-delivered si-RNA transduction to knockdown Zbtb7a in AM (as described in Fig. 2A), a 30-day intrabronchial anti-H-$2K^d$ administration was conducted to elicit OAD. In si-scramble huCD68-K^d Tg C57BL/6 lungs, anti-H-$2K^d$ induced intraluminal and peribronchiolar fibrosis, and *de novo* Abs and Th17 responses to Col V and Kα1T (Fig. 5B–E).

The Zbtb7a-deficient lungs (si-Zbtb7a transduced), in contrast, exhibited intact bronchiolar architecture with non-obstructed lumen and reduced Col V and Kα1T specific immune responses in response to anti-H-$2K^d$ (Fig. 5D–E). To assess the role(s) of AM in anti-MHC pathogenesis as an antigen-presenting cell, expression of surface MHC class II and co-stimulatory molecules were analyzed in response to anti-H-$2K^d$ (Fig. 5F). The huCD68-K^d Tg C57BL/6 AMs with intact Zbtb7a expression exhibited an activated phenotype with greater cell surface expression of I-A^b and CD40, indicating an increased antigen-presenting ability compared to that of Zbtb7a-deficient AMs. The effect of Zbtb7a deficiency on the phagocytic properties of AM was further evaluated; however, no noticeable differences were observed in AMs from untreated, si-scramble, and si-Zbtb7a groups as they were capable of dextran endocytosis and latex bead phagocytosis at equivalent rates regardless of their Zbtb7a expressions (sFig. 4A–B).

To further understand the pathogenesis of MHC ligation and to investigate the protective effects of Zbtb7a knockdown in Ab-induced OAD, we analyzed a detailed panel of molecules involved in anti-inflammation, granulocyte growth, leukocyte traffic, vesicular mobilization and cytoskeletal stability, and remodeling of ECM (sFig. 5). Consistent with earlier observations of anti-MHC ligation, Zbtb7a was significantly upregulated in huCD68-K^d Tg C57BL/6 lungs following anti-H-$2K^d$ administration. Furthermore, Zbtb7a deficiency resulted in a higher expression of anti-inflammatory molecule (*i.e.*leukemia inhibitory factor, an anti-inflammatory molecule (63)) concomitant with a significant reduction in T cell, B cell, and neutrophil chemoattractants (chemokine C-C motif ligand 27a, Cxcl11, Cxcl13, Cxcl15) (59, 60, 64, 65). In addition, Zbtb7a-sufficient lungs induced a higher expression of Col V (Col5a1), the core component of collagen fibrillogenesis (66), whereas Zbtb7a-deficient lungs produced greater amounts of ECM remodeling and cytoskeletal stabilizing factors.

Requirement of Zbtb7a signaling in elicitation of AM directed alloimmunity

We evaluated the influence of Zbtb7a deficiency on the development of spontaneous allogeneic responses and OAD following an adoptive AM transfer. In our earlier study, transfer of single antigen mismatched AM resulted in Ab and T cell responses to the mismatched AM antigen and autoimmunity to lung-restricted SAgs and OAD (36). The

purpose of the present study on intrabronchial transfer of AMs (si-scramble or si-Zbtb7a transduced) into Zbtb7a-sufficient or Zbtb7a-deficient lungs was to assess the significance of donor and recipient Zbtb7a signaling in the allogeneic AM-induced immune responses. Transfer of huCD68-K^d Tg AMs (unmodified and si-scramble transduced) into Zbtb7a-sufficient lungs elicited higher anti-H-$2K^d$ titers (Fig. 6A). In contrast, transfer of Zbtb7a-deficient AMs into Zbtb7a-sufficient lungs and vice versa resulted in lower titers (nearly 50% reduction in median fluorescence intensity [MFI]). However, complete resolution of the anti-H-$2K^d$ titer (~95% MFI decline) was achieved when both the donor AM and recipient lungs were Zbtb7a-deficient. Additionally, induction of alloimmune (H-$2K^d$ reactive) Th17 cells exhibited a similar trend where Zbtb7a knockdown in both donor and recipient registered a maximum reduction compared to other AM transfer combinations (Fig. 6B). This interruption of Zbtb7a signaling (either in the donor or the recipient) interfering in the development of alloAbs and alloimmune T cells indicated a Zbtb7a-dependency in elicitation of AM-directed alloimmunity. Furthermore, the protective effects of Zbtb7a-deficiency in donor and recipient were additive where double knockdown (in donor as well as in recipient) induced near-complete abrogation of AM-directed immune responses.

Reduced production of donor-derived exosomes by Zbtb7a-deficient AMs

Nanovesicular/exosome-mediated trafficking of donor-derived antigen is recognized in the allorecognition of transplanted antigens (67). We evaluated the influence of Zbtb7a on the production of H-$2K^{d+}$ exosomes following allogeneic transfer huCD68-K^d Tg AMs into C57BL/6 recipients (from Fig. 6). Using anti-CD63 coated beads, optimized in our earlier study (68), total exosomes in cell-free BAL fluid were positively identified for staining with exosome-specific marker where composition of the Siglec-F+ (AM-derived) exosomes were further analyzed for the alloantigen-containing exosomes (*i.e.*H-$2K^d$). Although the total exosomes found in BAL fluid did not differ significantly between the AM transfer groups (Fig. 7A), production of allogeneic exosomes by Zbtb7a-deficient donor AM was markedly lower, constituting ~5% of the exosome pool compared with ~21% in the Zbtb7a-sufficent donor AMs (Fig. 7B). Zbtb7a deficiency in the recipient AM, although it resulted in a marginal decline in total BAL exosomes, did not affect the allo-exosome production. The reduction of H-$2K^{d+}$ exosome preponderance associated with donor Zbtb7a deficiency may be indicative of a lower availability and/or transfer of the donor-derived antigens in the alloimmune sensitization.

Impaired antigen presentation and T cell proliferation by Zbtb7a-deficient AM

To obtain insight into possible impairment in the antigen-processing ability of Zbtb7a-deficient AMs that did not induce alloimmunity (Fig. 6), we co-transferred antigen-pulsed AM and T cell receptor-transgenic T cells into naïve recipients. Proliferation of OT-II T cell receptor transgenic T cells (I-A^b restricted chicken ova albumin 323–339 specific) was measured by carboxyfluorescein succinimidyl ester dilution in the lungs as well as in the spleen following intrabronchial transfer of AMs primed with latex bead (L)-coated ova albumin (L-OVA) or bovine serum albumin (L-BSA) or OVA 323–339 peptide. The OT-II T cells proliferated in lungs that received L-OVA or OVA 323–339 loaded to Zbtb7a-sufficient AMs (*i.e.*si-scramble treated). Furthermore, co-transfer of Zbtb7a-deficient AMs pulsed with whole protein antigen or the T cell epitope peptide failed to induce proliferation of OT-II

cells. Impaired T cell proliferation (Fig. 8) along with reduced AM-directed alloimmunity (Fig. 6) following Zbtb7a knockdown is indicative of a Zbtb7a-dependent antigen presenting cell function for AM, and suggests an important role for AM in the *in vivo* priming of alloantigen and lung-restricted SAg-reactive T cells.

Discussion

Despite significant advances in pre- and postoperative care since the first human LTx in 1963, CR remains the primary obstacle to successful LTx (4). Studies have postulated that immunologic priming directed at mismatched donor HLA initiates a cascade of immune responses to lung-restricted SAgs, resulting in CR—clinically diagnosed as BOS (8, 69, 70). The number of HLA mismatches between a lung graft donor and the recipient (71) and an early appearance of DSA (12) are strong risk factors for CR. A significant clinical association between *de novo* DSA and graft rejection has been demonstrated; however, a lack of understanding of the early mediators and key regulators in DSA-induced lung inflammation has hindered the understanding of—and possible intervention for—Ab-induced CR. In our preclinical murine model, ligation of surface MHC by specific Abs elicited OAD, a clinical correlate of BOS in humans (18, 19). We utilized the OAD model to identify and characterize early inflammation that transpires post-MHC ligation in an attempt to decipher the pathogenic roles of Abs. Because the OAD model necessitated exogenous Ab administration to the lung milieu without interference of immunosuppression, it afforded us unperturbed access to kinetic studies at molecular and cellular levels that is currently not feasible in any experimental models of CR, including the orthotopic murine LTx (72, 73).

Gene microarray assay followed by functional validations identified Zbtb7a as an early indicator and a critical modulator in anti-MHC pathogenesis. Strikingly, the LTxRs who developed *de novo* DSA and BOS exhibited greater induction of ZBTB7A compared to those who remained BOS-free (Fig. 3). This finding is particularly meaningful considering the lack of a viable molecular marker that predicts BOS. Classification of BOS requires a clinical assessment with forced expiratory volume 1 decline >20% of baseline (74), although recently CR has been described as chronic lung allograft dysfunction (CLAD) that includes both restrictive and obstructive lung diseases (*i.e.*restrictive allograft syndrome and BOS, respectively) (75). Induction of ZBTB7A as early as six months post-transplant in LTxRs who developed obstructive bronchiolitis and localization of ZBTB7A to AMs, offers prognostic significance since the half-life ($t^{1/2}$) of lung allografts remains as low as five years, and the progressive decline in pulmonary function at diagnosis of CLAD is an irreversible and untreatable phenomenon. As there is no gold standard for diagnosis of acute rejection (AR) following LTx, we were unable to identify significance of ZBTB7A in LTxRs suspected of Ab-mediated AR. Furthermore, the kinetics of ZBTB7A expression were positively associated with development of post-LTx DSA (Fig. 3D). This implies an inducible ZBTB7A in response to DSA that correlates with the experimental OAD wherein anti-MHC stimulates Zbtb7a induction (Fig. 1). The alloimmune B cell priming and/or the initial Ab production likely happen in the lung microenvironment where the presence of B cells and T cells at the graft rejection site (51) and local production of class-switched Abs have been documented (76–79). As systemic Abs could not be evaluated in mouse OAD model where anti-MHC is sequestered en route before reaching the lung tissue, we assessed

lung Zbtb7a induction in allogeneic mouse orthotopic LTx model. Systemic administration of Ab to allogeneic MHC particularly induced Zbtb7a in the transplanted lung allograft (sFig. 6). Therefore, DSA (whether *de novo* developed or experimentally introduced locally or systemically) is capable of inducing Zbtb7a in the lungs.

Interruption of gene function by si-RNA resulted in a persistent decline of Zbtb7a expression in the lungs. With less accumulation of lung-trophic B cells and neutrophils in si- Zbtb7a transduced lungs, anti-MHC failed to induce pulmonary inflammation, autoimmunity, and OAD (Fig. 2, sFig. 2). Appearance of "early" neutrophil and "late" B cell accumulations are considered key cellular responses—*albeit* non-specific—to MHC ligation, as B cells have an obligatory role in airway obliteration (56) and neutrophils regulate development of secondary lymphoid clusters consistent with iBALT (55). Additionally, a concurrent decrease in the Col V- and Kα1T-reactive IL-17 and IFN-γ producing cells further confirmed establishment of an "anti-inflammatory state" associated with the loss of Zbtb7a. Further, we observed Zbtb7a induction in lymphopenic mice following MHC ligation (sFig. 7). Since anti-H-2K^b resulted in Zbtb7a upregulation, non-lymphoid cells in lungs, without participation of lymphocytes, were sufficient to induce Zbtb7a in response to anti-MHC. AM was the predominant cell type responsible for lung Zbtb7a expression (Fig. 4A,C). Stimulation of Zbtb7a in primary murine and human AM cultures by MHC ligations (Fig. 4B) implies Zbtb7a induction as an early response to Abs. Development of OAD and lung-restricted, SAgs-directed autoimmunity (Fig. 5B–E) following MHC class I ligation on huCD68-K^d Tg C57BL/6 AM was a proof of concept that demonstrated a key role for AM in the anti-MHC pathogenesis. Furthermore, the downstream effector functions of AM were Zbtb7a-dependent since its targeted disruption ameliorated bronchiolar occlusion and reduced exacerbation of lung-restricted autoimmunity (Fig. 5B–C).

We propose two key roles for AM in Ab-mediated lung graft rejection. 1) As an early responder to Abs, AM shapes the local inflammatory milieu through recruitment and/or production of cellular and soluble mediators, and 2) serves as an initiator of the Ab response by directly modulating B cell and T cell responses. Intrabronchial instillation of anti-H-2K^b and anti-H-2K^d in Zbtb7a-sufficient C57BL/6 and huCD68-K^d Tg C57BL/6 mice, respectively, has satisfied the early responder role(s) that elicited cellular and humoral autoimmune responses and induced OAD, whereas the role of AM as an initiator of alloimmunity (*i.e.*DSA) has been established where transfer of MHC mismatched AM elicited systemic and local alloAbs and alloimmune T cells (36, 77, 78).

The current study focused on characterization of molecular mechanisms critical in the initiation and amplification of AM-induced DSA responses. While AMs are professional phagocytes (80, 81), naïve AMs in non-inflamed lungs are poor antigen presenters due to a lack of sufficient co-stimulation (82), whereas AMs function as efficient antigen-presenting cells upon pulmonary infection, vaccination, or transplantation (30, 33, 34, 83). Uninterrupted Zbtb7a signaling induced the antigen presentation ability of AMs in response to MHC ligation by stimulating greater MHC class II (I-A^b) and co-stimulatory molecule (CD40) expression. The Zbtb7a-deficient AMs, in contrast, did not exhibit such stimulations —indicating their diminished capacity for antigen presentation. Intrabronchial transfer of Zbtb7a-deficient allogeneic AMs in to Zbtb7a-sufficient lungs or vice versa also resulted in

a decrease in AM directed alloAbs and activation of alloimmune T cells (Fig. 6, sTable 3). To elucidate this reduced immunogenicity of Zbtb7a-deficient AMs, intercellular transfer of transplant antigen via exosomes was evaluated. Exosome-mediated passage of donor antigens into recipient's antigen-presenting cells has been recognized in semi-direct and indirect alloimmune sensitization (67), and exosomes produced by antigen-presenting cells (e.g., macrophage and dendritic cells) are known to be inflammatory (84, 85). We have shown an association of donor-derived exosomes with lung graft rejection (68). The exosomes from LTxRs experiencing lung graft rejection contained donor HLA molecules, but exosomes from stable LTx recipients did not. Demonstration of a ~75% decrease in the Zbtb7a-deficient donor AM-produced allo-exosomes (Fig. 7B) indicates a reduced availability of transferable alloantigen, and along with diminished antigen presentation (Fig. 5F, sTable 4), it correlates with reduced alloimmunity of Zbtb7a deficiency in donor AMs (Fig. 6). However, a complete abrogation of alloimmune priming was achieved when both the donor and recipient AMs were Zbtb7a-deficient (Fig. 6). Additionally, the Zbtb7a-deficient AMs were unable to stimulate antigen-specific T cell proliferation (Fig. 8). Taken together, protection from Ab-induced lung inflammation achieved by selective loss of Zbtb7a in the AM was multifactorial where Zbtb7a deficiency stimulated anti-inflammatory signals, dampened pro-inflammatory and pro-fibrotic signals, produced lesser allo-exosomes, and ultimately rendered AM as an inefficient antigen-presenting cell.

The present study documents the complexity of MHC Ab-induced pathogenesis in which an early and unique transcriptional landscape regulated airway inflammation, autoimmunity and remodeling of airways, ultimately leading to chronic small airway obstruction. An early induction of Zbtb7a, localized to lung-resident AMs, was an indicator and important mediator in the anti-MHC disease development. Overall, Ab ligation of MHC class I on AM cell surface stimulated an early entry of inflammatory cells into lung milieu and development of a "conditioned state" for subsequent priming and expansion of lung-restricted autoimmunity. Given the long-term persistence of allogeneic donor AMs in the transplanted lungs (36, 37), the efficacy of local ZBTB7A disruption needs to be evaluated in BOS prevention in LTxRs. Because B cell priming and production of *de novo* DSA precedes detectable serum DSA, and because BAL analysis is standard post-LTx care across transplant centers, evaluation of AM ZBTB7A may serve as an early indicator for post-LTx DSA and CR, and may measure the efficacy of DSA-directed therapies.

Methods

Mice and Ab-induced OAD

Wild-type C57BL/6 mice (6–8 wks, male) were procured from Charles River Laboratories (Frederick, MD), $Rag1^{-/-}$ mice were obtained from The Jackson Laboratory (Bar Harbor, ME), and Rag2/OT-II mice were from Taconic Biosciences (Hudson, NY). C57BL/6 mice that express H-$2K^d$ transgene on macrophage (huCD68-K^d Tg C57BL/6 mice) were described earlier (62). Mice were maintained at Washington University School of Medicine according to institutional guidelines and approved protocols. For induction of OAD, anti-H-$2K^b$ (AF6-88.5.5.3, BioXcell, West Lebanon, NH), anti-H-$2K^d$ (SF1.1.10, BioXcell) or isotype control (C1.18.4, BioXcell) Abs tested for being endotoxin-free (<2 EU/mg protein

determined by LAL gel clotting test) were administered intrabronchially as described earlier (18). Briefly, 200 μg of Ab (40 μL) was instilled through a 22G catheter on days 1, 2, 3 and 6 and weekly thereafter. Histopathologic evaluation of lung tissue sections was assessed by H&E and Massons' Trichrome staining. The images were captured by Aperio VERSA scanner (1.0.2.3.8; Leica Biosystems, Buffalo Grove, IL) and analyzed by Aperio ImageScope (v12.3.2.5030, Leica Biosystems).

Microarray analysis

Lung transcriptome was analyzed after intrabronchial administration of anti-H-2K^b or isotype control on days one, two, three and six. The lungs were harvested at 4 h post-Ab administration and perfused with low endotoxin phosphate buffered saline (PBS, pH 7.4; Thermo Fisher Scientific) (3×10 mL) to deplete circulating blood cells. The superior lobe from the left lung was stored in RNALater (Thermo Fisher Scientific) and total RNA was extracted by PureLink RNA kit (Thermo Fisher Scientific) followed by DNase I (Thermo Fisher Scientific) treatment. RNA quality was determined by gel-chip image (showing 28S, 18S and 5S bands) and RNA integrity number ([RIN], generally a RIN >7 indicates good quality RNA) using an Agilent 2100 Bioanalyzer (Agilent, Palo Alto, CA). All RNA preparations had RIN scores ≥ 7. Total RNA concentration was obtained from an absorbance ratio at 260nm and 280nm using a NanoDrop ND-100 spectrometry instrument (NanoDrop Inc., Wilmington, DE). Microarray assays were carried out at the Genome Technology Access Center at Washington University. Briefly, full-length mRNA was enriched by MessageAmpII aRNA Amplification kit (ThermoFisher Scientific) and reverse-transcribed into cDNA according to the manufacturer's protocol. cDNAs were chemically labeled with a Kreatech ULS RNA labeling kit (Kreatech Diagnostics) and Cy5-labeled cDNAs were hybridized to Agilent Mouse v2 4×44K microarrays (G4846A-026655). Slides were scanned on an Agilent C-class Microarray scanner. Gridding and analysis of images were performed using Feature Extraction (v11.5.1.1, Agilent Technologies).

In the Feature Extraction exported data files, rProcessed signal and rIsWellAboveBG parameters were imported into Partek Genome Suite (version 6.6, Partek Inc., Saint Louis, MO) for initial data QC followed by statistical analysis. Of the 39,429 array probes, 23,789 were detectable and were used in downstream differential expression analysis. These 23,789 probes were filtered by rIsWellAboveBG detection calls (exercised at 2 of the 24 samples called "detected"). Analysis of variance (ANOVA) was performed in Partek Genome Suite to identify differentially expressed genes between control and treated samples. The initial *p*-values from ANOVA analysis were corrected by false discovery rate method (FDR, or q-value) (86).

Lentivirus transduction

Zbtb7a-targeted knockdown was achieved by a lentiviral delivery of si-RNA targeting four sequences (sFig. 2A) on mouse Zbtb7a. Lentiviruses with si-Zbtb7a (iV036281) and scrambled si-RNA (LVP015-G) were obtained from Applied Biological Materials, Inc. (Richmond, BC, Canada). Briefly, the si-RNAs were cloned into piLenti-siRNA-GFP vector and replication-deficient pantropic lentivirus particles were produced with VSV-G as envelope protein. The *in vivo* transduction was performed according to Wilson et al. (54). In

brief, mice were anesthetized with Ketamine/Xylazine cocktail (100mg/Kg body) and si-RNA lentivirus (10^7 infectious units per mouse) was delivered intrabronchially. Three days post-lentivirus transduction, mice were infused with Abs for OAD development.

ELISA, ELISPOT and Western blot

Mouse Abs to lung-restricted SAgs were detected by our ELISA protocol (18). Briefly, ELISA plates were coated with recombinant Col V or Kα1T proteins (100ng/well) and detection of the specific Abs in serum was done by probing with HRP-conjugated goat anti-mouse IgG (Jackson Immunoresearch Laboratories, West Grove, PA). Analyses of donor-specific HLA Abs, and Col V or Kα1T autoantibodies in LTxRs were earlier described (87). Ab specificity was ascertained by competitive inhibition with addition of free Ag (100× molar excess) to the serum samples that inhibited Ab binding to ELISA wells. Estimation of SAg-specific Th1, Th2, Th17 and Treg cells in the lungs was conducted by quantifying cytokine (IFN-γ, IL-4, IL-17A and IL-10)-secreting ELISPOT assays (BD Biosciences, San Jose, CA and eBioscience, San Diego, CA) following our earlier optimized protocol with modification (18). Single cell suspension was prepared from PBS-perfused lungs by digestion with Liberase TL (300μg/mL, Roche Life Science, Indianapolis, IN) and DNaseI (5U/mL, Sigma-Aldrich, Saint Louis, MO) at 37°C for 25 min.

The lung digests were filtered through 100μM membrane and washed thrice in PBS supplemented with fetal bovine serum (2%) and EDTA (2 mM), after which leukocytes were isolated by Ficoll-Paque (Sigma-Aldrich) gradient centrifugation and resuspended at 1×10^7/mL in CTL-Test medium (Cellular Technology Limited, Shaker Heights, OH) for use in ELISPOT assay. One million lung leukocytes were added per well and were supplemented with 5×10^4 C57BL/6 splenocytes (irradiated at 30 Gy) as antigen-presenting cells. The cells were primed with recombinant Col V and Kα1T protein at 1μg/mL and cytokine-producing spots were enumerated by CTL-Immunospot analyzer (Cellular Technology Limited). Enumeration of alloreactive (H-2K^d specific) and autoreactive (H-2K^b specific) T cells was conducted by stimulating splenocytes from recipient mice with irradiated (30Gy) T cells (EasySep mouse T cell isolation kit, Stemcell Technologies; Vancouver, BC, Canada) from Balb/c and C57BL/6, respectively, following our established protocol (36). For Western blot analysis, lung tissue was lysed in radioimmunoprecipitation assay lysis buffer (Santa Cruz Biotechnology, Dallas, Texas) with protease inhibitors. The lysates (10μg protein equivalent) were electrophoresed on 4%–12% gradient SDS-polyacrylamide gel, then blotted onto polyvinylidene fluoride membrane and probed with anti-Zbtb7a (clone 466407; R&D Systems, Minneapolis, MN) or anti-β-Actin (clone C4, Santa Cruz Biotechnology).

LTxRs and sampling strategy

Human studies were approved by the Institutional Review Board at Washington University, and LTxRs gave consent for enrollment in the study. We retrospectively identified a total of 139 patients who underwent primary bilateral LTx at Barnes-Jewish Hospital/Washington University School of Medicine (BJC/WU) between January 2009 and December 2013. Routine care for LTxRs at BJC/WU includes follow-up visits at one, two, three, six and twelve months and then yearly post-transplant visits (unless more are needed for clinical reasons).

Blood, needle biopsy and BAL fluid were collected in clinic during follow-up visits as a standard procedure, and cellular profiles of BAL fluid at the time of collection were obtained from the patients' charts. Serum and PBL were fractionated from whole blood. BAL cells were isolated by centrifugation at 1500×g for 10min at 4°C and stored in RNA later at −80°C. We evaluated 21 LTxRs who developed BOS and compared them with a time-matched cohort of 21 LTxRs with stable pulmonary function with no evidence of rejection. DSA was determined using LABScreen single antigen assay (ThermoFisher Scientific, Waltham, MA) and Abs to lung-restricted SAgs (Col V and Kα1T) were determined using ELISA developed in our laboratory (87).

We retrospectively analyzed LTxRs who developed BOS and those remained BOS-free (stable) at three, six and 12 months post-LTx. LTxRs who developed *de novo* DSA (MFI >2000) received Ab-directed therapy (*i.e.*intravenous Ig and rituximab) and the matched post-LTx BAL samples were stratified as pre-DSA, DSA-peaked, DSA-reduced, and DSA-resolved based on their serum MFI for DSA. The LTxRs who did not develop DSA (DSA negative) had no episodes of rejection and did not develop *de novo* Abs to Col V and Kα1T, and remained stable without any decrease in pulmonary function. We further evaluated elicitation of DSA in combination with *de novo* Abs to lung-restricted SAgs (*i.e.*Col V and Kα1T).

Reverse transcription and quantitative PCR analyses

Reverse transcription PCR was performed on cDNAs synthesized from total RNA with amplification parameters: 94°C 2min followed by 30 cycles of 94°C 30sec, 55°C 30sec and 68°C 90sec with a final extension 68°C 10min. DNA polymerase (Platinum Pfx) was from ThermoFisher Scientific and following oligonucleotide pairs were synthesized by Integrated DNA Technologies (Coralville, IA)- Zbtb7a: TGGCCTGAGAGAGATGAAGA/ GCTTGTCCTGTCTGGTGAAT; Scgb1a1: ACATCTGCCCAGGATTTCTTC/ TCTTGCTTACACAGAGGACTTG; Cxcl13: CGGTATTCTGGAAGCCCATTAC/ TCAGGCAGCTCTTCTCTTACT; Cxcl15: CACTCAAGAGCTACGATGTCTG/ TCCCGAATTGGAAAGGGAAATA; Mmp2: GTTCAACGGTCGGGAATACA/ TGTCACTGTCCGCCAAATAA; Mmp9: TCTGTATGGTCGTGGCTCTA/ CCTGTAATGGGCTTCCTCTATG; ActB: GAGGTATCCTGACCCTGAAGTA/ GCTCGAAGTCTAGAGCAACATAG.

Quantitative PCR was performed on total RNA isolated from the lung tissue, BAL cells, and purified AMs, and was reverse-transcribed with Superscript first strand synthesis (ThermoFisher Scientific). The primers/probes were obtained from Integrated DNA Technologies: for mouse-Zbtb7a (Mm.PT.58.29517580), Zbtb7b (Mm.PT.58.10467993), Lifr (Mm.PT.58.13542050), Cxcl11 (Mm.PT.58.42838989), Cxcl13 (Mm.PT.58.31389616), Cxcl15 (Mm.PT.58.9981538), Ccl27 (Mm.PT.58.12096426.g), Csf2 (Mm.PT.58.9186111), Cx3cr1 (Mm.PT.58.17555544), Col5a1 (Mm.PT.58.31056233), Ccbe1 (Mm.PT. 58.6423596), Hook3 (Mm.PT.58.13030313), Tppp (Mm.PT.58.11880654), Reck (Mm.PT. 58.13897726), Myo5a (Mm.PT.56a.28745598), Map1b (Mm.PT.58.30879382), Actb (Mm.PT.58.33540333) and for humans- ZBTB7A (Hs.PT.58.39675134), CD68 (Hs.PT. 58.2488447.g), PPARG (Hs.PT.58.25464465), ACTB (Hs.PT.39a.22214847). Amplification

was performed with TaqMan Fast Advanced Master Mix (ThermoFisher Scientific) in CFX Connect Real-Time PCR Detection System (Bio-Rad Laboratories, Hercules, CA). Target gene expression was normalized with appropriate housekeeping genes and quantified by $2^{-\Delta\Delta ct}$ method (88).

Isolation of mouse BAL fluid and respiratory epithelial cells

Mouse BAL fluid was collected via a 22G catheter installed into the trachea followed by five subsequent washes (1 mL/wash) with ice-chilled Ca^{+2} and Mg^{+2} free PBS with EDTA (1mM). The BAL cells were pelleted by centrifugation at 250 ×g at 4°C for 10min. Isolation of mouse respiratory epithelial cells was performed according to the methods described by Lam et al. (89). Briefly, after collection of BAL cells, the lungs were digested overnight by 0.15% pronase (Sigma-Aldrich) digestion at 4°C, and the epithelial cells were harvested following DNaseI treatment.

Flow cytometry and cell sorting

Single-cell suspension from the lungs was prepared by digestion with Liberase TL as described earlier in Methods. Cells were Fc blocked (clones 2.4G2 and 93) to saturate CD16/CD32-mediated non-specific binding. The following Abs were utilized in flow cytometry for mouse cells: CD45-PE/Cy7 (I3/2.3), CD4-PE (GK1.5), CD8b-APC (YTS156.7.7), CD19-PerCP/Cy5.5 (6D5), B220- APC/Cy7 (RA3-6B2), CD11b-APC/Cy7 or Brilliant Blue 515 (M1/70), CD11c-Alexa Fluor 488 or eFluor450 (N418), Siglec-F-Brilliant violet 421 (E50-2440) and Ly-6G/C (Gr-1)-Brilliant violet 510 (RB6-8C5), H-$2K^b$-APC (AF6-88.5), H-$2K^d$-PE (SF1-1.1), F4/80-APC/Cy7 (BM8), I-A^b-PE/Cy7 (AF6-120.1), CD80- PerCP/Cy5.5 (16-10A1), CD40- Brilliant violet 510 (1C10). For staining human cells, CD45-Alexa Fluor 488 (HI30), CD11b-PE/Cy7 (M1/70), HLA DR-APC/Cy7 (L243), CD169-APC (7-239), CD15-Brilliant Violet 510 (W6D3), CD163-Brilliant Violet 421 (GHI/61) and CD206-PE (15-2) were used. Abs were purchased from BD Biosciences, Biolegend (San Diego, CA) or eBioScience. Stained cells were fixed with neutral buffered paraformaldehyde (2%) before being analyzed by BD FACSCanto II cell analyzer (BD Biosciences). AMs were isolated from BAL cells. Human AMs were identified as CD45+, HLA-DR+, CD15-, CD11b+, CD206+, CD169+ and CD163+ BAL cells, whereas the AMs in mice were characterized as CD45+, CD11c+, Siglec-F+, F4/80+/- CD11b- BAL cells (36). The AM fractions were enriched (>95% purity) by a BD FACS Aria II cell sorter (BD Biosciences), and the non-AM BAL cells were also collected. AlloAbs (H-$2K^d$ specific) were analyzed by staining mouse T cells (EasySep mouse T cell isolation kit, Stemcell Technologies). Flow cytometry data were analyzed by FlowJo 10.0 (Tree Star).

Culture of AM

Freshly isolated human and mouse AMs were cultured respectively in RPMI 1640 (ThermoFisher Scientific) or DMEM (ThermoFisher Scientific) supplemented with 10% FBS and 20% L-929 culture supernatant (as source of M-CSF, 100 U/mL final concentration) and seeded in 12-well plate at 1×10^6 cells/well as described (36). Ab ligation of surface MHC was by addition of 100 μg/mL anti-H-$2K^b$ (AF6-88.5.5.3, IgG2a) or anti-I-A/I-E (M5/114, IgG2b) to mouse AMs and anti-HLA (W6/32, IgG2a) to human AMs, and the responses to MHC ligation were compared with that of isotype matched

immunoglobulins (C.1.18.4, IgG2a or LTF-2, IgG2b). Ligation of keratin (a cell-surface, non-MHC molecule) by anti-keratin (AE3, IgG1) was also evaluated. Thirty minutes prior to Ab stimulation, cells were incubated with Fc block (clones 2.4G2 and 93 for mouse AMs and Human BD Fc Block for human AMs) at 2μg/mL and the Fc block was maintained at 2μg/mL during the experiment. The cells were cultured at 37°C at 6% CO_2 for 4h and harvested for mRNA analysis.

Isolation and analysis of BAL exosome

Exosome isolation and analysis were carried out as per our described protocol (68). Briefly, exosomes from cell-free BAL fluid were precipitated by ExoQuick-TC (System Biosciences, Palo Alto, CA). The total protein quantification and enumeration of exosomes from BAL fluid were performed by FluoroProfile Protein Quantification Kit (Sigma-Aldrich) and a FluoroCet kit (System Biosciences), respectively, according to manufacturer's guidelines. Anti-CD63 coated beads (Exo-Flow, System Biosciences) were used to capture exosomes, and bead-bound exosomes were analyzed for exosome-specific staining (Exo-APC, System Biosciences) by LSRFortessa X-20 (BD Biosciences) flow cytometer. Positive staining with anti-Siglec-F (an AM specific marker) was done to ascertain cellular origin, and staining with anti-H-2K^d and anti-H-2K^b were done to distinguish the origin (*i.e.*donor vs recipient) for BAL fluid exosomes.

Adoptive transfer and proliferation of T cells

Aldehyde/Amidine latex beads (1.5μ, ThermoFisher Scientific) were conjugated with OVA or BSA according to manufacturer's protocol and were maintained at a final concentration of 1% solid that contained 0.95–1.02μg protein/μL. The antigen-coated beads delivering 5μg protein, or 1μg of OVA323-339 peptide (AnaSpec, Fremont, CA) were intrabronchially administered into lungs 6h before collection of BAL fluid. The antigen-pulsed donor AMs (purified as described earlier) were intrabronchially transferred (1×10^5 cells per mouse, >99% viable) into C57BL/6 recipients. Naïve OVA-specific CD4 T cells isolated from Rag2/OT-II spleen (EasySep mouse CD4+ T cell enrichment kit, Stemcell Technologies; Vancouver, BC, Canada) and labeled with carboxyfluorescein diacetate succinimidyl ester (CFSE, 5μM; ThermoFisher Scientific) were intravenously transferred at 5×10^6/mouse immediately following the AM transfer. Proliferation of OT-II T cells was measured by CFSE dilution in lungs and spleen at 72 h post-transfer.

Orthotopic murine LTx

Orthotopic vascularized left LTx was performed using cuff techniques with Balb/c donors and C57BL/6 recipients (90). All recipients were treated with anti-CD154 (MR1, 250μg on day 0 postoperatively; BioXcell), and CTLA4-Ig (200μg on day 2 post operative, BioXCell) to induce allograft acceptance (72). On day 28 post-LTx, anti-H-2K^d (200μg, SF1.1.10) was administered intraperitoneally, and the native lung, transplanted lung, peripheral blood leukocytes and splenocytes from the LTxR mice were harvested for analysis after 6h.

Statistical analysis

All results are presented as mean ± SEM, and ANOVA, multiple, paired or un-paired t tests were used to evaluate statistical significance. Study designs, sample sizes with biological replicates, and statistical analyses are indicated in respective experiments. $p<0.05$ was considered statistically significant. Data were analyzed and plotted with Prism 7.0 (GraphPad Software, Inc., La Jolla, CA).

Study approval

Mice experiments were approved by the Animal Studies Committee at Washington University, and were performed using institutional guidelines and approved protocols. Blood, BAL fluid, and lung biopsy specimens were collected from LTxRs at routine visits as a standard protocol for evaluating the clinical status. The human LTxRs provided consent, and the Institutional Review Board at Washington University approved the studies.

Supplementary Material

Refer to Web version on PubMed Central for supplementary material.

Acknowledgments

We thank Clare Prendergast and Billie Glasscock for assistance with manuscript editing, and Marco Marchionni for assistance with illustration.

Funding: This research was supported by a grant from Flinn Foundation awarded to DKN and MAS (#2095), and grants from National Institutes of Health awarded to TM (R01HL056643 and R01HL092514) and MT (R01AI102891).

References

1. Djamali A, Kaufman DB, Ellis TM, Zhong W, Matas A, Samaniego M. Diagnosis and management of antibody-mediated rejection: current status and novel approaches. American journal of transplantation : official journal of the American Society of Transplantation and the American Society of Transplant Surgeons. 2014; 14:255–271.
2. Kobashigawa JA. Continuing the pursuit of heart transplant antibody-mediated rejection. The Journal of heart and lung transplantation : the official publication of the International Society for Heart Transplantation. 2015; 34:1134–1135.
3. Hachem RR. Lung allograft rejection: diagnosis and management. Curr Opin Organ Transplant. 2009; 14:477–482. [PubMed: 19617825]
4. Kotloff RM, Thabut G. Lung transplantation. American journal of respiratory and critical care medicine. 2011; 184:159–171. [PubMed: 21471083]
5. Hachem RR, Yusen RD, Meyers BF, Aloush AA, Mohanakumar T, Patterson GA, Trulock EP. Anti-human leukocyte antigen antibodies and preemptive antibody-directed therapy after lung transplantation. The Journal of heart and lung transplantation : the official publication of the International Society for Heart Transplantation. 2010; 29:973–980.
6. Ius F, Sommer W, Tudorache I, Kuhn C, Avsar M, Siemeni T, Salman J, Hallensleben M, Kieneke D, Greer M, Gottlieb J, Haverich A, Warnecke G. Early donor-specific antibodies in lung transplantation: risk factors and impact on survival. The Journal of heart and lung transplantation : the official publication of the International Society for Heart Transplantation. 2014; 33:1255–1263.
7. Morrell MR, Pilewski JM, Gries CJ, Pipeling MR, Crespo MM, Ensor CR, Yousem SA, D'Cunha J, Shigemura N, Bermudez CA, McDyer JF, Zeevi A. De novo donor-specific HLA antibodies are associated with early and high-grade bronchiolitis obliterans syndrome and death after lung

transplantation. The Journal of heart and lung transplantation : the official publication of the International Society for Heart Transplantation. 2014; 33:1288–1294.

8. Saini D, Weber J, Ramachandran S, Phelan D, Tiriveedhi V, Liu M, Steward N, Aloush A, Hachem R, Trulock E, Meyers B, Patterson GA, Mohanakumar T. Alloimmunity-induced autoimmunity as a potential mechanism in the pathogenesis of chronic rejection of human lung allografts. The Journal of heart and lung transplantation : the official publication of the International Society for Heart Transplantation. 2011; 30:624–631.
9. Todd JL, Palmer SM. Bronchiolitis obliterans syndrome: the final frontier for lung transplantation. Chest. 2011; 140:502–508. [PubMed: 21813529]
10. Jaramillo A, Smith MA, Phelan D, Sundaresan S, Trulock EP, Lynch JP, Cooper JD, Patterson GA, Mohanakumar T. Development of ELISA-detected anti-HLA antibodies precedes the development of bronchiolitis obliterans syndrome and correlates with progressive decline in pulmonary function after lung transplantation. Transplantation. 1999; 67:1155–1161. [PubMed: 10232567]
11. Palmer SM, Davis RD, Hadjiliadis D, Hertz MI, Howell DN, Ward FE, Savik K, Reinsmoen NL. Development of an antibody specific to major histocompatibility antigens detectable by flow cytometry after lung transplant is associated with bronchiolitis obliterans syndrome. Transplantation. 2002; 74:799–804. [PubMed: 12364858]
12. Le Pavec J, Suberbielle C, Lamrani L, Feuillet S, Savale L, Dorfmuller P, Stephan F, Mussot S, Mercier O, Fadel E. De-novo donor-specific anti-HLA antibodies 30 days after lung transplantation are associated with a worse outcome. The Journal of heart and lung transplantation : the official publication of the International Society for Heart Transplantation. 2016; 35:1067–1077.
13. Baskaran G, Tiriveedhi V, Ramachandran S, Aloush A, Grossman B, Hachem R, Mohanakumar T. Efficacy of extracorporeal photopheresis in clearance of antibodies to donor-specific and lung-specific antigens in lung transplant recipients. The Journal of heart and lung transplantation : the official publication of the International Society for Heart Transplantation. 2014; 33:950–956.
14. Ius F, Sommer W, Tudorache I, Kuhn C, Avsar M, Siemeni T, Salman J, Hallensleben M, Kieneke D, Greer M, Gottlieb J, Kielstein JT, Boethig D, Welte T, Haverich A, Warnecke G. Preemptive treatment with therapeutic plasma exchange and rituximab for early donor-specific antibodies after lung transplantation. The Journal of heart and lung transplantation : the official publication of the International Society for Heart Transplantation. 2015; 34:50–58.
15. Tinckam KJ, Keshavjee S, Chaparro C, Barth D, Azad S, Binnie M, Chow CW, de Perrot M, Pierre AF, Waddell TK, Yasufuku K, Cypel M, Singer LG. Survival in sensitized lung transplant recipients with perioperative desensitization. American journal of transplantation : official journal of the American Society of Transplantation and the American Society of Transplant Surgeons. 2015; 15:417–426.
16. Bharat A, Saini D, Steward N, Hachem R, Trulock EP, Patterson GA, Meyers BF, Mohanakumar T. Antibodies to self-antigens predispose to primary lung allograft dysfunction and chronic rejection. Ann Thorac Surg. 2010; 90:1094–1101. [PubMed: 20868794]
17. Tiriveedhi V, Gautam B, Sarma NJ, Askar M, Budev M, Aloush A, Hachem R, Trulock E, Myers B, Patterson AG, Mohanakumar T. Pre-transplant antibodies to Kalpha1 tubulin and collagen-V in lung transplantation: clinical correlations. The Journal of heart and lung transplantation : the official publication of the International Society for Heart Transplantation. 2013; 32:807–814.
18. Fukami N, Ramachandran S, Saini D, Walter M, Chapman W, Patterson GA, Mohanakumar T. Antibodies to MHC class I induce autoimmunity: role in the pathogenesis of chronic rejection. Journal of immunology (Baltimore, Md. 1950). 2009; 182:309–318.
19. Takenaka M, Tiriveedhi V, Subramanian V, Hoshinaga K, Patterson AG, Mohanakumar T. Antibodies to MHC class II molecules induce autoimmunity: critical role for macrophages in the immunopathogenesis of obliterative airway disease. PLoS One. 2012; 7:e42370. [PubMed: 22900015]
20. Guilliams M, De Kleer I, Henri S, Post S, Vanhoutte L, De Prijck S, Deswarte K, Malissen B, Hammad H, Lambrecht BN. Alveolar macrophages develop from fetal monocytes that differentiate into long-lived cells in the first week of life via GM-CSF. The Journal of experimental medicine. 2013; 210:1977–1992. [PubMed: 24043763]

21. Hoeffel G, Chen J, Lavin Y, Low D, Almeida FF, See P, Beaudin AE, Lum J, Low I, Forsberg EC, Poidinger M, Zolezzi F, Larbi A, Ng LG, Chan JK, Greter M, Becher B, Samokhvalov IM, Merad M, Ginhoux F. C-Myb(+) erythro-myeloid progenitor-derived fetal monocytes give rise to adult tissue-resident macrophages. Immunity. 2015; 42:665–678. [PubMed: 25902481]
22. Perdiguero GE, Klapproth K, Schulz C, Busch K, Azzoni E, Crozet L, Garner H, Trouillet C, de Bruijn MF, Geissmann F, Rodewald HR. Tissue-resident macrophages originate from yolk-sac-derived erythro-myeloid progenitors. Nature. 2015; 518:547–551. [PubMed: 25470051]
23. Schneider C, Nobs SP, Kurrer M, Rehrauer H, Thiele C, Kopf M. Induction of the nuclear receptor PPAR-gamma by the cytokine GM-CSF is critical for the differentiation of fetal monocytes into alveolar macrophages. Nat Immunol. 2014; 15:1026–1037. [PubMed: 25263125]
24. Hussell T, Bell TJ. Alveolar macrophages: plasticity in a tissue-specific context. Nat Rev Immunol. 2014; 14:81–93. [PubMed: 24445666]
25. Kopf M, Schneider C, Nobs SP. The development and function of lung-resident macrophages and dendritic cells. Nat Immunol. 2015; 16:36–44. [PubMed: 25521683]
26. Stone KC, Mercer RR, Gehr P, Stockstill B, Crapo JD. Allometric relationships of cell numbers and size in the mammalian lung. Am J Respir Cell Mol Biol. 1992; 6:235–243. [PubMed: 1540387]
27. Westphalen K, Gusarova GA, Islam MN, Subramanian M, Cohen TS, Prince AS, Bhattacharya J. Sessile alveolar macrophages communicate with alveolar epithelium to modulate immunity. Nature. 2014; 506:503–506. [PubMed: 24463523]
28. Davies LC, Jenkins SJ, Allen JE, Taylor PR. Tissue-resident macrophages. Nat Immunol. 2013; 14:986–995. [PubMed: 24048120]
29. Ghoneim HE, Thomas PG, McCullers JA. Depletion of alveolar macrophages during influenza infection facilitates bacterial superinfections. Journal of immunology (Baltimore, Md. 1950). 2013; 191:1250–1259.
30. Hartwig SM, Holman KM, Varga SM. Depletion of alveolar macrophages ameliorates virus-induced disease following a pulmonary coronavirus infection. PLoS One. 2014; 9:e90720. [PubMed: 24608125]
31. Pribul PK, Harker J, Wang B, Wang H, Tregoning JS, Schwarze J, Openshaw PJ. Alveolar macrophages are a major determinant of early responses to viral lung infection but do not influence subsequent disease development. J Virol. 2008; 82:4441–4448. [PubMed: 18287232]
32. Schneider C, Nobs SP, Heer AK, Kurrer M, Klinke G, van Rooijen N, Vogel J, Kopf M. Alveolar macrophages are essential for protection from respiratory failure and associated morbidity following influenza virus infection. PLoS Pathog. 2014; 10:e1004053. [PubMed: 24699679]
33. Benoit A, Huang Y, Proctor J, Rowden G, Anderson R. Effects of alveolar macrophage depletion on liposomal vaccine protection against respiratory syncytial virus (RSV). Clinical and experimental immunology. 2006; 145:147–154. [PubMed: 16792685]
34. Macdonald DC, Singh H, Whelan MA, Escors D, Arce F, Bottoms SE, Barclay WS, Maini M, Collins MK, Rosenberg WM. Harnessing alveolar macrophages for sustained mucosal T-cell recall confers long-term protection to mice against lethal influenza challenge without clinical disease. Mucosal Immunol. 2014; 7:89–100. [PubMed: 23715172]
35. Sekine Y, Bowen LK, Heidler KM, Van Rooijen N, Brown JW, Cummings OW, Wilkes DS. Role of passenger leukocytes in allograft rejection: effect of depletion of donor alveolar macrophages on the local production of TNF-alpha, T helper 1/T helper 2 cytokines, IgG subclasses, and pathology in a rat model of lung transplantation. Journal of immunology (Baltimore, Md. 1950). 1997; 159:4084–4093.
36. Nayak DK, Zhou F, Xu M, Huang J, Tsuji M, Hachem R, Mohanakumar T. Long-term persistence of donor alveolar macrophages in human lung transplant recipients that influences donor specific immune responses. American journal of transplantation : official journal of the American Society of Transplantation and the American Society of Transplant Surgeons. 2016; 16:2300–2311.
37. Eguiluz-Gracia I, Schultz HH, Sikkeland LI, Danilova E, Holm AM, Pronk CJ, Agace WW, Iversen M, Andersen C, Jahnsen FL, Baekkevold ES. Long-term persistence of human donor alveolar macrophages in lung transplant recipients. Thorax. 2016

38. Maeda T, Hobbs RM, Merghoub T, Guernah I, Zelent A, Cordon-Cardo C, Teruya-Feldstein J, Pandolfi PP. Role of the proto-oncogene Pokemon in cellular transformation and ARF repression. Nature. 2005; 433:278–285. [PubMed: 15662416]

39. Lunardi A, Guarnerio J, Wang G, Maeda T, Pandolfi PP. Role of LRF/Pokemon in lineage fate decisions. Blood. 2013; 121:2845–2853. [PubMed: 23396304]

40. Maeda T, Ito K, Merghoub T, Poliseno L, Hobbs RM, Wang G, Dong L, Maeda M, Dore LC, Zelent A, Luzzatto L, Teruya-Feldstein J, Weiss MJ, Pandolfi PP. LRF is an essential downstream target of GATA1 in erythroid development and regulates BIM-dependent apoptosis. Dev Cell. 2009; 17:527–540. [PubMed: 19853566]

41. Maeda T, Merghoub T, Hobbs RM, Dong L, Maeda M, Zakrzewski J, van den Brink MR, Zelent A, Shigematsu H, Akashi K, Teruya-Feldstein J, Cattoretti G, Pandolfi PP. Regulation of B versus T lymphoid lineage fate decision by the proto-oncogene LRF. Science (New York, N.Y.). 2007; 316:860–866.

42. Sakurai N, Maeda M, Lee SU, Ishikawa Y, Li M, Williams JC, Wang L, Su L, Suzuki M, Saito TI, Chiba S, Casola S, Yagita H, Teruya-Feldstein J, Tsuzuki S, Bhatia R, Maeda T. The LRF transcription factor regulates mature B cell development and the germinal center response in mice. The Journal of clinical investigation. 2011; 121:2583–2598. [PubMed: 21646720]

43. Carpenter AC, Grainger JR, Xiong Y, Kanno Y, Chu HH, Wang L, Naik S, dos Santos L, Wei L, Jenkins MK, O'Shea JJ, Belkaid Y, Bosselut R. The transcription factors Thpok and LRF are necessary and partly redundant for T helper cell differentiation. Immunity. 2012; 37:622–633. [PubMed: 23041065]

44. Reis BS, Rogoz A, Costa-Pinto FA, Taniuchi I, Mucida D. Mutual expression of the transcription factors Runx3 and ThPOK regulates intestinal CD4(+) T cell immunity. Nat Immunol. 2013; 14:271–280. [PubMed: 23334789]

45. Vacchio MS, Wang L, Bouladoux N, Carpenter AC, Xiong Y, Williams LC, Wohlfert E, Song KD, Belkaid Y, Love PE, Bosselut R. A ThPOK-LRF transcriptional node maintains the integrity and effector potential of post-thymic CD4+ T cells. Nat Immunol. 2014; 15:947–956. [PubMed: 25129370]

46. Kukita A, Kukita T, Ouchida M, Maeda H, Yatsuki H, Kohashi O. Osteoclast-derived zinc finger (OCZF) protein with POZ domain, a possible transcriptional repressor, is involved in osteoclastogenesis. Blood. 1999; 94:1987–1997. [PubMed: 10477728]

47. Tsuji-Takechi K, Negishi-Koga T, Sumiya E, Kukita A, Kato S, Maeda T, Pandolfi PP, Moriyama K, Takayanagi H. Stage-specific functions of leukemia/lymphoma-related factor (LRF) in the transcriptional control of osteoclast development. Proceedings of the National Academy of Sciences of the United States of America. 2012; 109:2561–2566. [PubMed: 22308398]

48. St-Jean JR, Ounissi-Benkalha H, Polychronakos C. Yeast one-hybrid screen of a thymus epithelial library identifies ZBTB7A as a regulator of thymic insulin expression. Molecular immunology. 2013; 56:637–642. [PubMed: 23911422]

49. Wang G, Lunardi A, Zhang J, Chen Z, Ala U, Webster KA, Tay Y, Gonzalez-Billalabeitia E, Egia A, Shaffer DR, Carver B, Liu XS, Taulli R, Kuo WP, Nardella C, Signoretti S, Cordon-Cardo C, Gerald WL, Pandolfi PP. Zbtb7a suppresses prostate cancer through repression of a Sox9-dependent pathway for cellular senescence bypass and tumor invasion. Nature genetics. 2013; 45:739–746. [PubMed: 23727861]

50. Masuda T, Wang X, Maeda M, Canver MC, Sher F, Funnell AP, Fisher C, Suciu M, Martyn GE, Norton LJ, Zhu C, Kurita R, Nakamura Y, Xu J, Higgs DR, Crossley M, Bauer DE, Orkin SH, Kharchenko PV, Maeda T. Transcription factors LRF and BCL11A independently repress expression of fetal hemoglobin. Science (New York, N.Y.). 2016; 351:285–289.

51. Sato M, Hirayama S, Hwang DM, Lara-Guerra H, Wagnetz D, Waddell TK, Liu M, Keshavjee S. The role of intrapulmonary de novo lymphoid tissue in obliterative bronchiolitis after lung transplantation. Journal of immunology (Baltimore, Md. 1950). 2009; 182:7307–7316.

52. Davies JM, Hawe N, Kabarowski J, Huang QH, Zhu J, Brand NJ, Leprince D, Dhordain P, Cook M, Morriss-Kay G, Zelent A. Novel BTB/POZ domain zinc-finger protein, LRF, is a potential target of the LAZ-3/BCL-6 oncogene. Oncogene. 1999; 18:365–375. [PubMed: 9927193]

53. Hirayama S, Sato M, Liu M, Loisel-Meyer S, Yeung JC, Wagnetz D, Cypel M, Zehong G, Medin JA, Keshavjee S. Local long-term expression of lentivirally delivered IL-10 in the lung attenuates

obliteration of intrapulmonary allograft airways. Human gene therapy. 2011; 22:1453–1460. [PubMed: 21568692]

54. Wilson AA, Murphy GJ, Hamakawa H, Kwok LW, Srinivasan S, Hovav AH, Mulligan RC, Amar S, Suki B, Kotton DN. Amelioration of emphysema in mice through lentiviral transduction of long-lived pulmonary alveolar macrophages. The Journal of clinical investigation. 2010; 120:379–389. [PubMed: 20038801]
55. Foo SY, Zhang V, Lalwani A, Lynch JP, Zhuang A, Lam CE, Foster PS, King C, Steptoe RJ, Mazzone SB, Sly PD, Phipps S. Regulatory T cells prevent inducible BALT formation by dampening neutrophilic inflammation. Journal of immunology (Baltimore, Md. 1950). 2015; 194:4567–4576.
56. Fukami N, Ramachandran S, Takenaka M, Weber J, Subramanian V, Mohanakumar T. An obligatory role for lung infiltrating B cells in the immunopathogenesis of obliterative airway disease induced by antibodies to MHC class I molecules. American journal of transplantation : official journal of the American Society of Transplantation and the American Society of Transplant Surgeons. 2012; 12:867–876.
57. Gelman AE, Li W, Richardson SB, Zinselmeyer BH, Lai J, Okazaki M, Kornfeld CG, Kreisel FH, Sugimoto S, Tietjens JR, Dempster J, Patterson GA, Krupnick AS, Miller MJ, Kreisel D. Cutting edge: Acute lung allograft rejection is independent of secondary lymphoid organs. Journal of immunology (Baltimore, Md. 1950). 2009; 182:3969–3973.
58. Rangel-Moreno J, Carragher DM, de la Luz Garcia-Hernandez M, Hwang JY, Kusser K, Hartson L, Kolls JK, Khader SA, Randall TD. The development of inducible bronchus-associated lymphoid tissue depends on IL-17. Nat Immunol. 2011; 12:639–646. [PubMed: 21666689]
59. Ansel KM, Harris RB, Cyster JG. CXCL13 is required for B1 cell homing, natural antibody production, and body cavity immunity. Immunity. 2002; 16:67–76. [PubMed: 11825566]
60. Chen SC, Mehrad B, Deng JC, Vassileva G, Manfra DJ, Cook DN, Wiekowski MT, Zlotnik A, Standiford TJ, Lira SA. Impaired pulmonary host defense in mice lacking expression of the CXC chemokine lungkine. Journal of immunology (Baltimore, Md. 1950). 2001; 166:3362–3368.
61. Iwata T, Chiyo M, Yoshida S, Smith GN Jr, Mickler EA, Presson R Jr, Fisher AJ, Brand DD, Cummings OW, Wilkes DS. Lung transplant ischemia reperfusion injury: metalloprotease inhibition down-regulates exposure of type V collagen, growth-related oncogene-induced neutrophil chemotaxis, and tumor necrosis factor-alpha expression. Transplantation. 2008; 85:417–426. [PubMed: 18322435]
62. Huang J, Li X, Kohno K, Hatano M, Tokuhisa T, Murray PJ, Brocker T, Tsuji M. Generation of tissue-specific H-2Kd transgenic mice for the study of K(d)-restricted malaria epitope-specific CD8+ T-cell responses in vivo. J Immunol Methods. 2013; 387:254–261. [PubMed: 23142461]
63. Hunt LC, Upadhyay A, Jazayeri JA, Tudor EM, White JD. An anti-inflammatory role for leukemia inhibitory factor receptor signaling in regenerating skeletal muscle. Histochem Cell Biol. 2013; 139:13–34. [PubMed: 22926285]
64. Ohneda O, Ohneda K, Nomiyama H, Zheng Z, Gold SA, Arai F, Miyamoto T, Taillon BE, McIndoe RA, Shimkets RA, Lewin DA, Suda T, Lasky LA. WECHE: a novel hematopoietic regulatory factor. Immunity. 2000; 12:141–150. [PubMed: 10714680]
65. Slight SR, Rangel-Moreno J, Gopal R, Lin Y, Fallert Junecko BA, Mehra S, Selman M, Becerril-Villanueva E, Baquera-Heredia J, Pavon L, Kaushal D, Reinhart TA, Randall TD, Khader SA. CXCR5(+) T helper cells mediate protective immunity against tuberculosis. The Journal of clinical investigation. 2013; 123:712–726. [PubMed: 23281399]
66. Sun M, Chen S, Adams SM, Florer JB, Liu H, Kao WW, Wenstrup RJ, Birk DE. Collagen V is a dominant regulator of collagen fibrillogenesis: dysfunctional regulation of structure and function in a corneal-stroma-specific Col5a1-null mouse model. J Cell Sci. 2011; 124:4096–4105. [PubMed: 22159420]
67. Alegre ML, Lakkis FG, Morelli AE. Antigen Presentation in Transplantation. Trends in immunology. 2016; 37:831–843. [PubMed: 27743777]
68. Gunasekaran M, Xu Z, Nayak DK, Sharma M, Hachem R, Walia R, Bremner RM, Smith MA, Mohanakumar T. Donor-Derived Exosomes With Lung Self-Antigens in Human Lung Allograft Rejection. American journal of transplantation : official journal of the American Society of Transplantation and the American Society of Transplant Surgeons. 2016

69. Seetharam A, Tiriveedhi V, Mohanakumar T. Alloimmunity and autoimmunity in chronic rejection. Curr Opin Organ Transplant. 2010; 15:531–536. [PubMed: 20613527]

70. Weber DJ, Wilkes DS. The role of autoimmunity in obliterative bronchiolitis after lung transplantation. American journal of physiology. Lung cellular and molecular physiology. 2013; 304:L307–311. [PubMed: 23262227]

71. Hayes D Jr, Black SM, Tobias JD, Kopp BT, Kirkby SE, Mansour HM, Whitson BA. Influence of human leukocyte antigen mismatching on bronchiolitis obliterans syndrome in lung transplantation. The Journal of heart and lung transplantation : the official publication of the International Society for Heart Transplantation. 2015

72. Okazaki M, Gelman AE, Tietjens JR, Ibricevic A, Kornfeld CG, Huang HJ, Richardson SB, Lai J, Garbow JR, Patterson GA, Krupnick AS, Brody SL, Kreisel D. Maintenance of airway epithelium in acutely rejected orthotopic vascularized mouse lung transplants. Am J Respir Cell Mol Biol. 2007; 37:625–630. [PubMed: 17717320]

73. Okazaki M, Krupnick AS, Kornfeld CG, Lai JM, Ritter JH, Richardson SB, Huang HJ, Das NA, Patterson GA, Gelman AE, Kreisel D. A mouse model of orthotopic vascularized aerated lung transplantation. American journal of transplantation : official journal of the American Society of Transplantation and the American Society of Transplant Surgeons. 2007; 7:1672–1679.

74. Meyer KC, Raghu G, Verleden GM, Corris PA, Aurora P, Wilson KC, Brozek J, Glanville AR. An international ISHLT/ATS/ERS clinical practice guideline: diagnosis and management of bronchiolitis obliterans syndrome. The European respiratory journal. 2014; 44:1479–1503. [PubMed: 25359357]

75. Verleden GM, Raghu G, Meyer KC, Glanville AR, Corris P. A new classification system for chronic lung allograft dysfunction. The Journal of heart and lung transplantation : the official publication of the International Society for Heart Transplantation. 2014; 33:127–133.

76. Bessa J, Jegerlehner A, Hinton HJ, Pumpens P, Saudan P, Schneider P, Bachmann MF. Alveolar macrophages and lung dendritic cells sense RNA and drive mucosal IgA responses. Journal of immunology (Baltimore, Md. 1950). 2009; 183:3788–3799.

77. Heidler KM, Baker K, Woods K, Schnizlein-Bick C, Cummings OW, Sidner R, Foresman B, Wilkes DS. Instillation of allogeneic lung antigen-presenting cells deficient in expression of major histocompatibility complex class I or II antigens have differential effects on local cellular and humoral immunity and on pathology in recipient murine lungs. Am J Respir Cell Mol Biol. 2000; 23:499–505. [PubMed: 11017915]

78. Wilkes DS, Heidler KM, Bowen LK, Quinlan WM, Doyle NA, Cummings OW, Doerschuk CM. Allogeneic bronchoalveolar lavage cells induce the histology of acute lung allograft rejection, and deposition of IgG2a in recipient murine lungs. Journal of immunology (Baltimore, Md. 1950). 1995; 155:2775–2783.

79. Wilkes DS, Sidner RA, Mathur PN, Niemeier M, Schwenk R, Heidler KM, Bowen LK. Preferential production of IgG2 antibodies by parenchymal lung B-lymphocytes during lung allograft rejection. Transplant Proc. 1997; 29:1891–1895. [PubMed: 9142313]

80. Jakubzick C, Tacke F, Llodra J, van Rooijen N, Randolph GJ. Modulation of dendritic cell trafficking to and from the airways. Journal of immunology (Baltimore, Md. 1950). 2006; 176:3578–3584.

81. MacLean JA, Xia W, Pinto CE, Zhao L, Liu HW, Kradin RL. Sequestration of inhaled particulate antigens by lung phagocytes. A mechanism for the effective inhibition of pulmonary cell-mediated immunity. The American journal of pathology. 1996; 148:657–666. [PubMed: 8579128]

82. Chelen CJ, Fang Y, Freeman GJ, Secrist H, Marshall JD, Hwang PT, Frankel LR, DeKruyff RH, Umetsu DT. Human alveolar macrophages present antigen ineffectively due to defective expression of B7 costimulatory cell surface molecules. The Journal of clinical investigation. 1995; 95:1415–1421. [PubMed: 7533793]

83. Nicod LP, Joudrier S, Isler P, Spiliopoulos A, Pache JC. Upregulation of CD40, CD80, CD83 or CD86 on alveolar macrophages after lung transplantation. The Journal of heart and lung transplantation : the official publication of the International Society for Heart Transplantation. 2005; 24:1067–1075.

84. Liu Q, Rojas-Canales DM, Divito SJ, Shufesky WJ, Stolz DB, Erdos G, Sullivan ML, Gibson GA, Watkins SC, Larregina AT, Morelli AE. Donor dendritic cell-derived exosomes promote allograft-

targeting immune response. The Journal of clinical investigation. 2016; 126:2805–2820. [PubMed: 27348586]

85. Singh PP, Smith VL, Karakousis PC, Schorey JS. Exosomes isolated from mycobacteria-infected mice or cultured macrophages can recruit and activate immune cells in vitro and in vivo. Journal of immunology (Baltimore, Md. 1950). 2012; 189:777–785.
86. Storey JD, Tibshirani R. Statistical significance for genomewide studies. Proceedings of the National Academy of Sciences of the United States of America. 2003; 100:9440–9445. [PubMed: 12883005]
87. Hachem RR, Tiriveedhi V, Patterson GA, Aloush A, Trulock EP, Mohanakumar T. Antibodies to K-alpha 1 tubulin and collagen V are associated with chronic rejection after lung transplantation. American journal of transplantation : official journal of the American Society of Transplantation and the American Society of Transplant Surgeons. 2012; 12:2164–2171.
88. Livak KJ, Schmittgen TD. Analysis of relative gene expression data using real-time quantitative PCR and the 2(-Delta Delta C(T)) Method. Methods (San Diego, Calif.). 2001; 25:402–408.
89. Lam HC, Choi AM, Ryter SW. Isolation of mouse respiratory epithelial cells and exposure to experimental cigarette smoke at air liquid interface. J Vis Exp. 2011
90. Krupnick AS, Lin X, Li W, Okazaki M, Lai J, Sugimoto S, Richardson SB, Kornfeld CG, Garbow JR, Patterson GA, Gelman AE, Kreisel D. Orthotopic mouse lung transplantation as experimental methodology to study transplant and tumor biology. Nature protocols. 2009; 4:86–93. [PubMed: 19131960]
91. Vandesompele J, De Preter K, Pattyn F, Poppe B, Van Roy N, De Paepe A, Speleman F. Accurate normalization of real-time quantitative RT-PCR data by geometric averaging of multiple internal control genes. Genome biology. 2002; 3 Research0034.

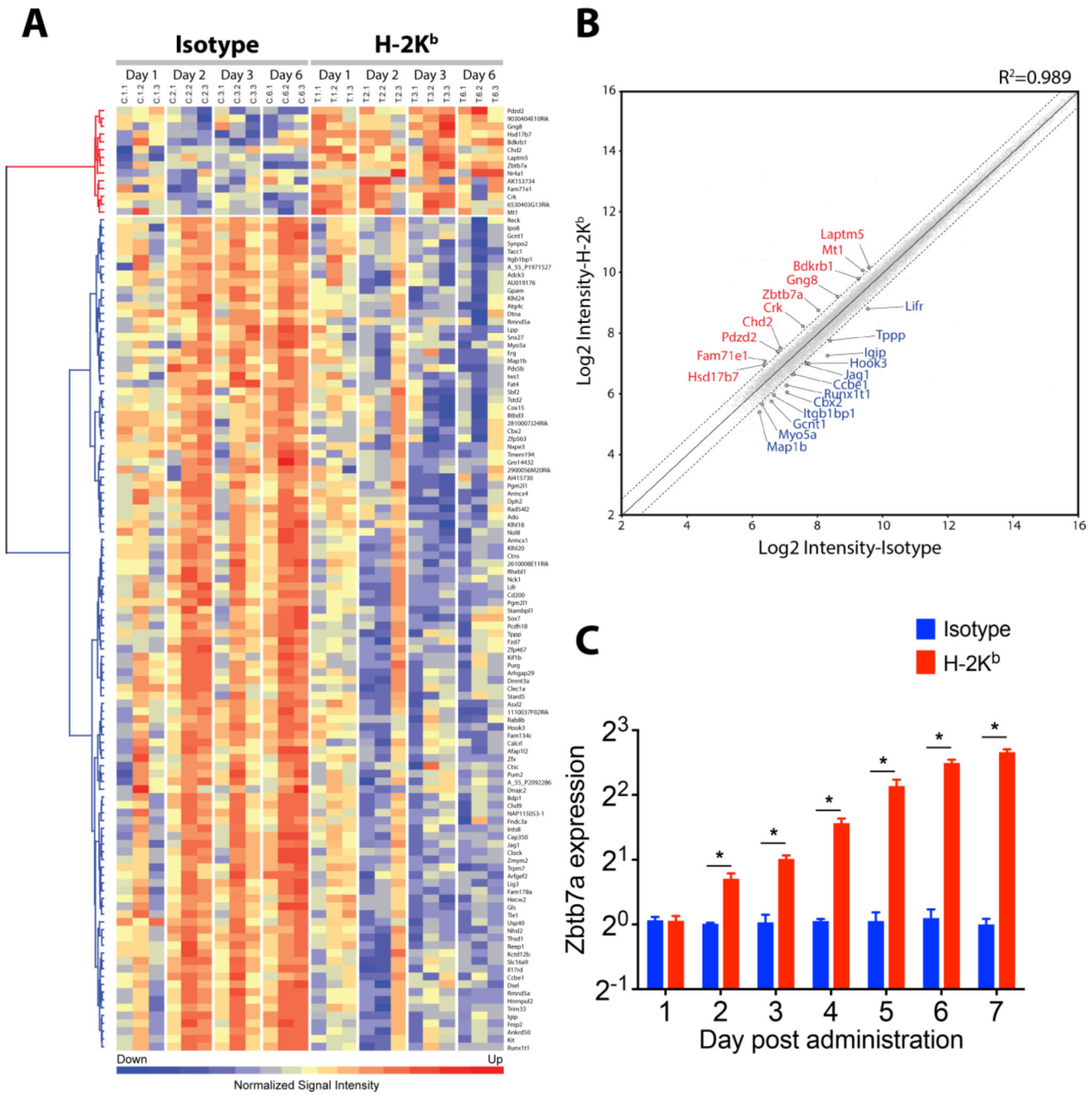

Fig. 1. Profile of the lung transcriptome following MHC class I ligation by specific Ab

(**A**) Heat map presentation of the differentially expressed genes following intrabronchial administration of H-2K^b or isotype control into C57BL/6 mice analyzed by mouse 4×44K mouse V2 chips (Agilent). Three mice per group per day were analyzed and plotted. Probe intensity was normalized by z-score, and red and blue color coding indicate higher and lower expression levels, respectively. Data have been deposited into the NCBI GEO database (GEO ID: GSE71426). (**B**) Scatterplot highlighting 23 selected genes differentially expressed between H-2K^b and isotype control groups. Mean signal intensities were transformed into Log2, and quantile normalization was applied. Differential expression was

determined by two-way ANOVA test, and expression level exceeding 1.5 fold, $p<0.05$ and FDR q<0.1 was deemed significant. The central solid line represents line of equality and genes expressed >1.5 fold demarcated by dashed lines are annotated (red: upregulated, blue: downregulated). (**C**) Quantitative PCR validation of Zbtb7a expression was conducted in a parallel experiment. Five mice per time point were analyzed for Zbtb7a expression (IDT assay id, Mm.PT.58.29517580) and normalized with that of Actb (IDT, Mm.PT. 58.33540333). Zbtb7a expression in untreated C57BL/6 lungs was set as baseline expression. Data are presented as mean±SEM, multiple t-test applied with multiple comparisons by Holm-Sidak method and $p<0.05$ is considered significant (*).

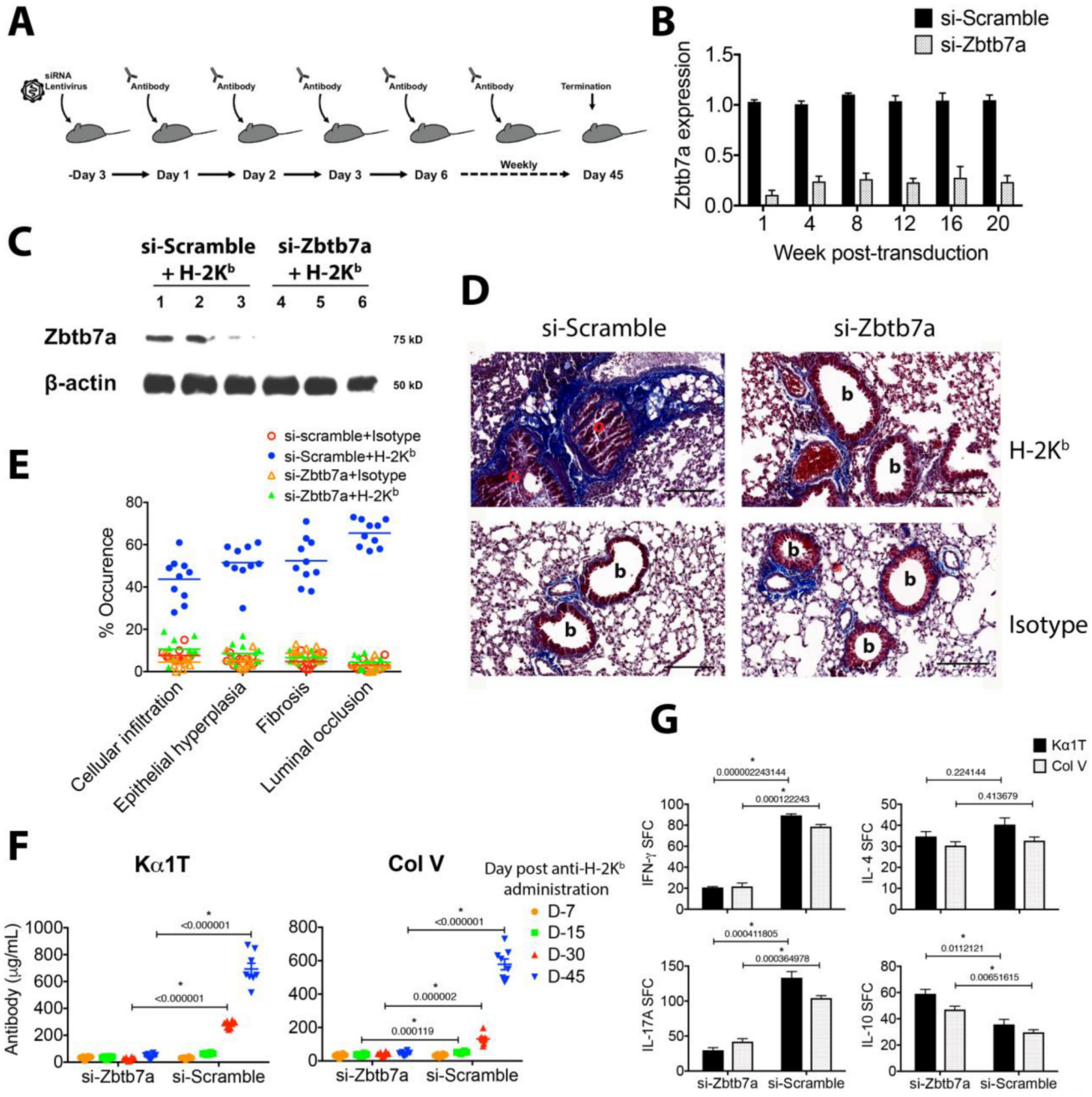

Fig. 2. Disruption of Zbtb7a expression in lungs prevents anti-MHC-induced lung-restricted autoimmunity and OAD

(**A**) Schematic representation of si-RNA lentivirus transduction and subsequent Ab challenges. Mice received an intrabronchial delivery of lentivirus (10^7 IU/mouse) three days prior to intrabronchial Ab regimen. (**B**) Repression in the Zbtb7a expression was quantified (as described in Fig. 1C). (**C**) Detection of Zbtb7a expression by Western blot analysis in lung lysates of three mice by anti-Zbtb7a (clone 466407) and anti-β-Actin (clone C4). (**D**) Representative Masson's trichrome staining on day 45 post-Ab administration. Fibrotic areas with deposition of collagenous ECM are stained blue, (b, bronchiole; o, occluded bronchiole). (**E**) Histopathologic score for each data point represents average of five fields

from each mouse (19). Median lines are drawn. (**F**) Titers for serum anti-Kα1T and -Col V were evaluated by ELISA from eight mice and mean±SEM lines are drawn. (**G**) Development of T cell autoreactivity was analyzed by ELISPOT on day 45. The data are presented as spot-forming cell (SFC) per million cells. Results are presented as mean±SEM. Multiple t-tests were applied with correction for Holm-Sidak method and significance of difference is marked (*p* values indicated). Scale bar in panel D is 100μm.

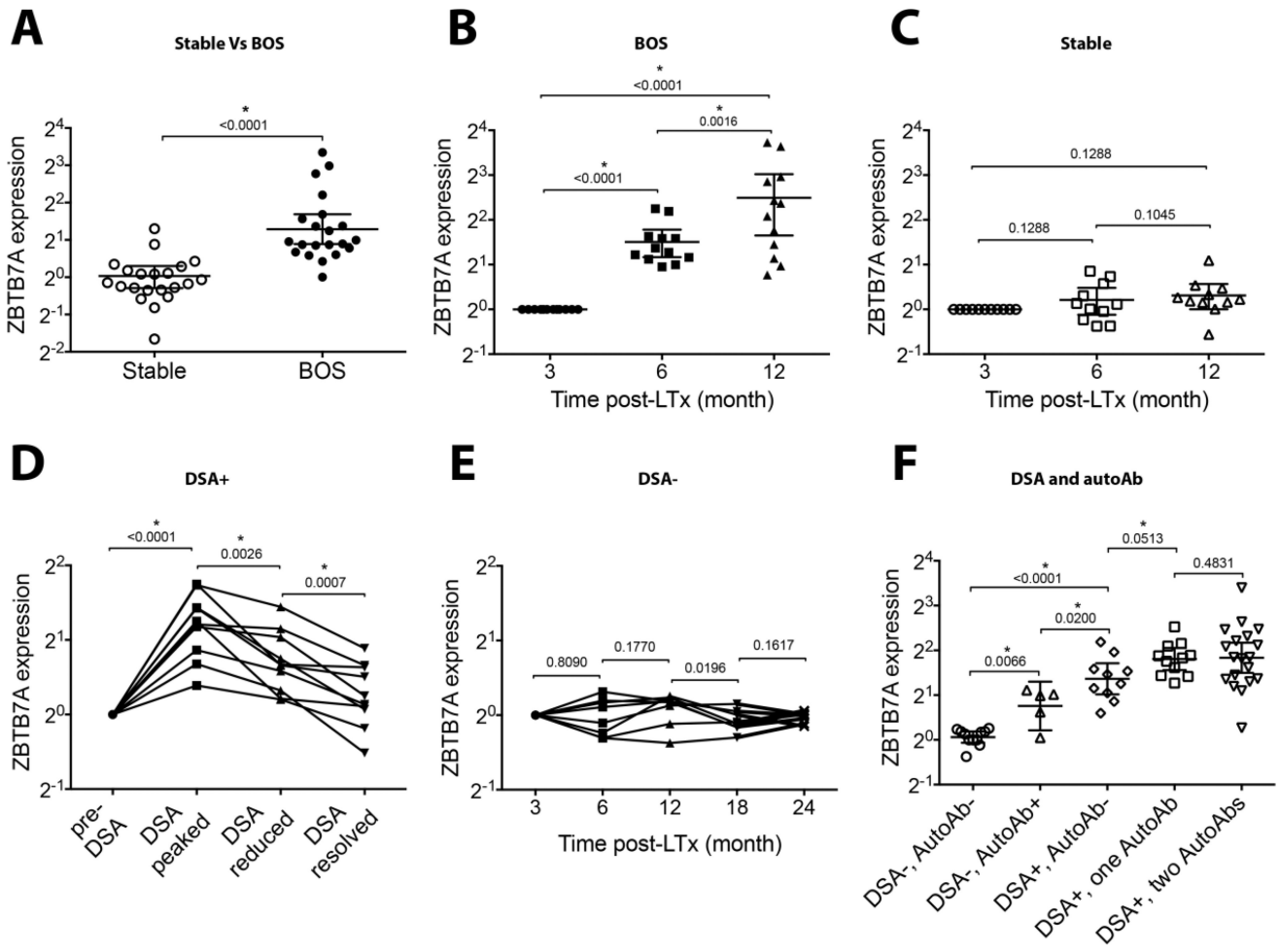

Fig. 3. Early induction of ZBTB7A in LTxRs who developed *de novo* DSA and BOS

BAL cell ZBTB7A expression was evaluated by quantitative PCR after normalization with ACTB, CD68, and PPARG (91). Delta Ct values at 3 months post-LTx were set as baseline for respective LTxRs (sTable 2), and relative expression for subsequent time points was calculated as $2^{-\Delta\Delta Ct}$. (**A**) ZBTB7A induction in a cohort of 21 BOS^+ LTxRs and time-matched 21 LTxRs who remained BOS-free, (**B**) kinetic study at 6±1 and 12±1 post-LTx months on 12 LTxRs who later developed BOS and (**C**) 11 LTxRs who remained stable were evaluated. (**D**) Ten LTxRs who developed *de novo* DSA (MFI >2000) and received Ab-directed therapies were stratified as pre-DSA (MFI<2000), DSA-peaked (highest MFI observed during follow-up of individual patient), DSA-reduced (2000<MFI<Peak), and DSA-resolved (MFI<2000). (**E**) Serial samples from eight stable LTxRs (DSA^- and not treated by Ab-directed therapies) were evaluated. (**F**) Role of DSA and autoAb (anti-Kα1T, anti-Col V) in ZBTB7A induction evaluated in LTxRs $DSA^-autoAb^-$ (n=11); $DSA^-autoAb^+$ (either anti-Kα1T or anti-Col V, n=5); $DSA^+autoAb^-$ (n=10); DSA^+one autoAb (either anti-Kα1T or anti-Col V, n=11) and DSA^+two autoAbs (anti-Kα1T and anti-Col V, n=19). Two-tailed Mann-Whitney U test was applied and *p* values are indicated. Significance of the results is marked at $p<0.05$ (*).

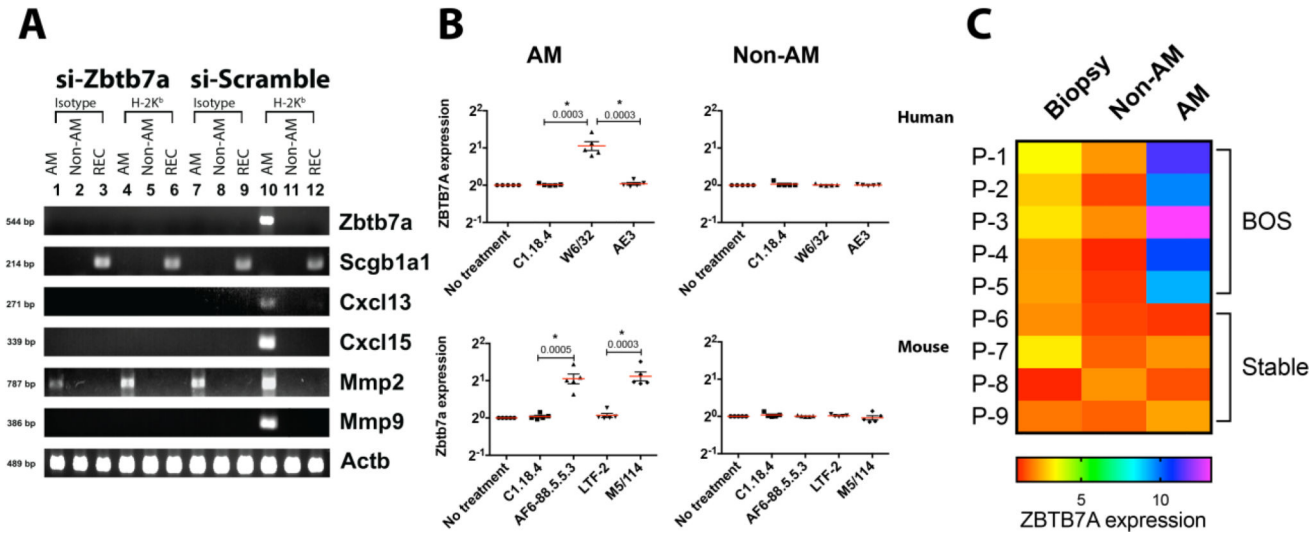

Fig. 4. Lung Zbtb7a induction in response to MHC ligations and in post-LTx BOS patients is localized to AMs

(**A**) Representative reverse transcription PCR analysis on total RNA isolated from BAL isolated AM (CD45+, CD11c+ and Siglec-F+) (lanes: 1, 4, 7 and 10), non-AM BAL cells (CD45+, CD11c- and Siglec-F-) (lanes: 2, 5, 8 and 11) and alveolar respiratory epithelial cells (REC, lanes: 3, 6, 9 and 12) on day seven from si-RNA lentivirus transduced and Ab-treated mice (n=6). (**B**) Freshly isolated human and mouse AMs were cultured at 1×10^6 cells per well, as previously described (36). Ligation of surface MHC class I was done by addition of anti-H-2K^b (clone AF6-88.5.5.3, IgG2a) and anti-HLA (W6/32, IgG2a) to mouse and human AMs, respectively. For ligation of MHC class II, anti-I-A/I-E (clone M5/114, IgG2b) was used. Responses to MHC ligation were compared with those of isotype controls (C. 1.18.4, IgG2a or LTF-2, IgG2b). Ligation of keratin was also evaluated by addition of anti-Keratin (AE3, IgG1). The final concentration of Abs were 100 μg/mL and cells were cultured at 37°C at 6% CO_2 for 4 h before mRNA analysis. Induction of Zbtb7a was normalized to that of Actb and presented as relative expression compared to untreated AMs. Data are presented as mean±SEM, two-tailed unpaired t-tests are applied, significance ($p<0.05$) is marked (*) and p values are indicated. (**C**) BAL cells from five BOS$^+$ LTxRs (P-1 through P-5) and four BOS-free LTxRs (P-6 through P-9) with stable lung function were fractionated into AM and non-AM as described earlier. The lung biopsy specimens were obtained on same day of BAL fluid collection. Fold induction in ZBTB7A expression compared to the peripheral blood leukocyte for individual LTxRs is plotted as heat map.

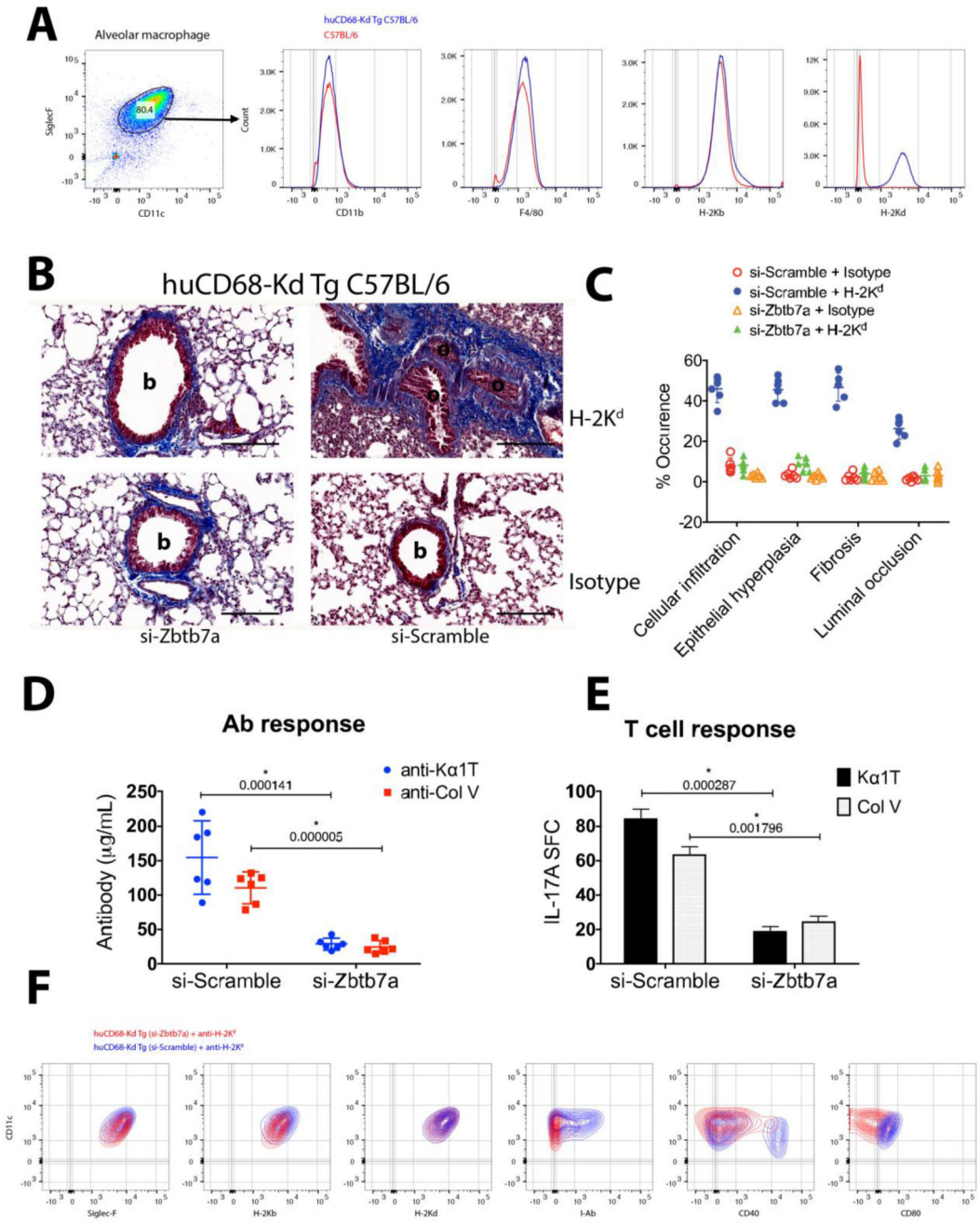

Fig. 5. Induction of lung-restricted autoimmunity and OAD by Ab ligation of AM MHC class I is Zbtb7a dependent

(**A**) AM surface expression of lineage markers and H-2K^d transgene in huCD68-K^d Tg C57BL/6. (**B**) Representative trichrome stained images showing fibrotic scar and occluded bronchiole in anti-H-2K^d induced OAD, day 30 (n=7) and (**C**) histopathology assessment of the OAD lesion. Development of *de novo* Ab titers (**D**) and stimulation of Th17 cells (**E**) specific for Kα1T and Col V were evaluated on day 30. (**F**) Surface expression of MHC (class I and II) and co-stimulatory molecules in Zbtb7a-sufficient or Zbtb7a-deficient AMs following anti-H-2K^d administration on day 30. Data were analyzed by multiple t-tests and

statistical significance (*) was determined using the Holm-Sidak method, with $p<0.05$. Scale bar in panel B is 100μm; b, bronchiole; o, occluded bronchiole.

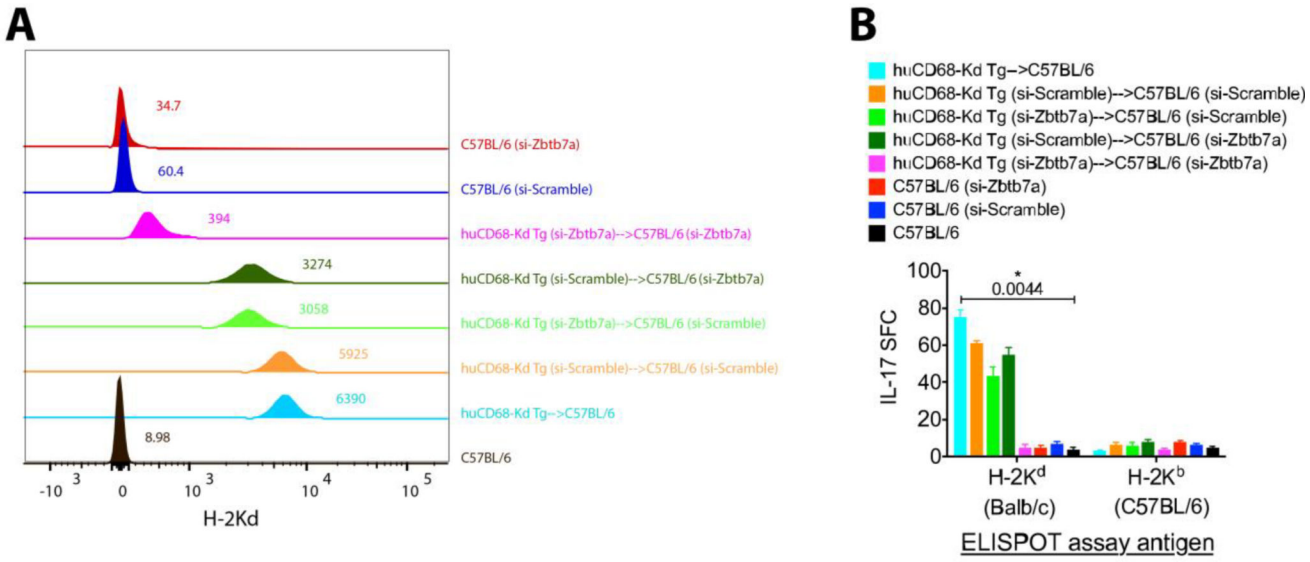

Fig. 6. Zbtb7a expression is essential in elicitation of AM-directed humoral and cellular alloimmunity

Allogeneic reconstitution of AM was by intrabronchial transfer of 4×10^5 huCD68-K^d Tg C57BL/6 AM into C57BL/6 recipients. Development of H-$2K^d$ specific Abs in BAL fluid (**A**) and lung-infiltrating Th17 cells in lungs (**B**) were measured respectively by flow cytometry and ELISPOT at 15 weeks by our earlier described protocol (36). Combinations of donor and recipient Zbtb7a knockdown were evaluated. Representative anti-H-$2K^d$ titers (in sTable 3) are presented as overlaid histograms (n=5–7) and individual MFI values are indicated. ELISPOT assay measured alloreactive (H-$2K^d$ specific) IL-17 producing cells per million lung leukocytes (mean±SEM) and one-way ANOVA was applied to test statistical significance (*).

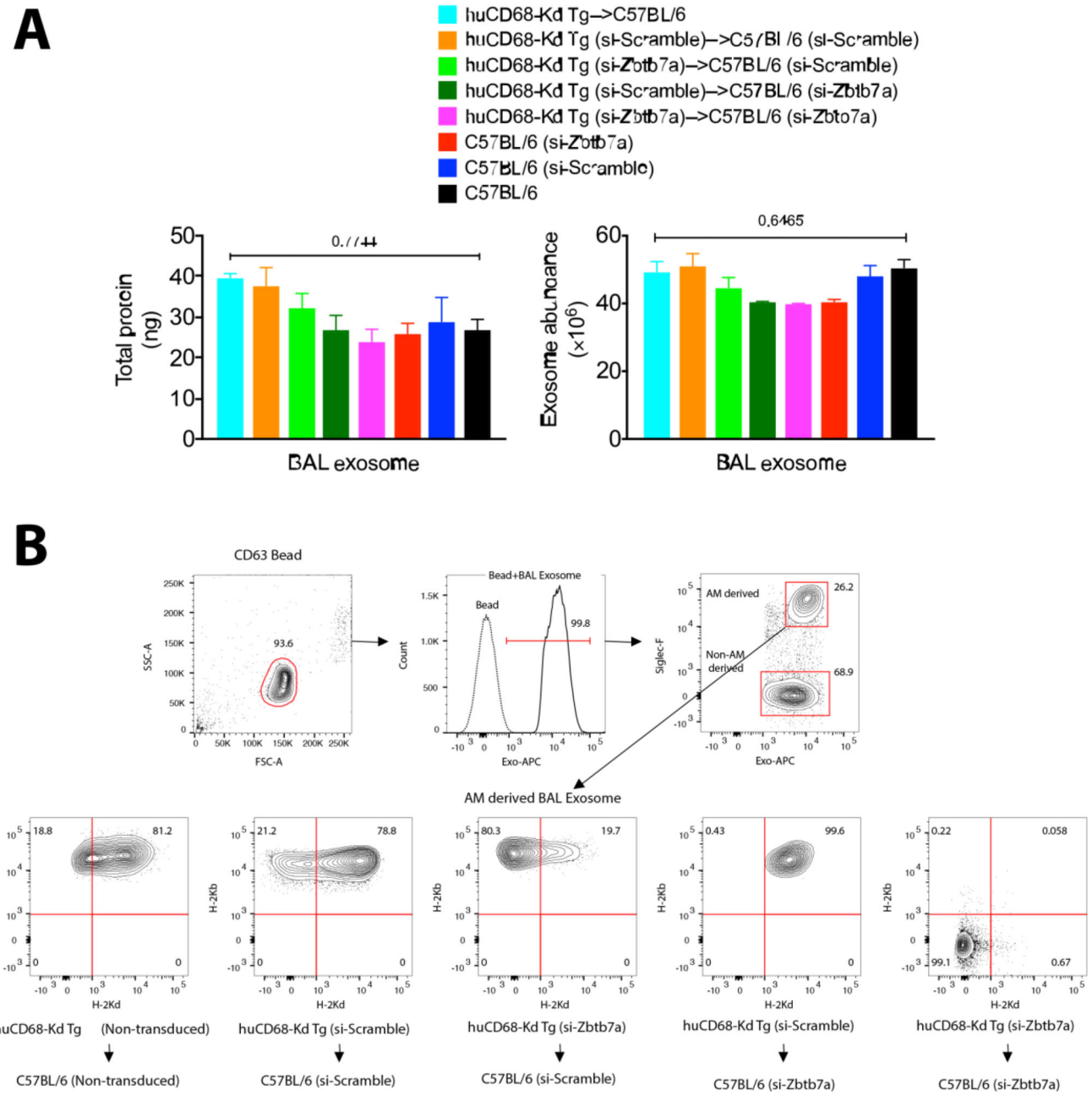

Fig. 7. Zbtb7a deficiency in donor AMs reduces donor-derived alloexosome production

(**A**) Quantitation of total exosomes isolated from cell-free BAL fluid following adoptive transfer of allogeneic AMs from Fig. 6. Data from three mice per AM transfer group were individually analyzed and presented as mean±SEM. One-way ANOVA was applied with Brown-Forsythe test that compares exosomes from the AM transfer groups with those from C57BL/6 as the baseline expression. Significance (*p* values) of differences is indicated. (**B**) Flow cytometric analysis of the BAL-derived exosomes was performed by anti-CD63 coated Exo-Flow magnetic beads. Exosomes bound to beads were positively identified by staining with Exo-APC. The AM-derived exosomes (Siglec-F^{+}) were analyzed for preponderance of

donor (for being H-2K^{d+} and H-2K^{b+}) or recipient (for being H-2K^{d-} and H-2K^{b+}) origin of BAL exosomes.

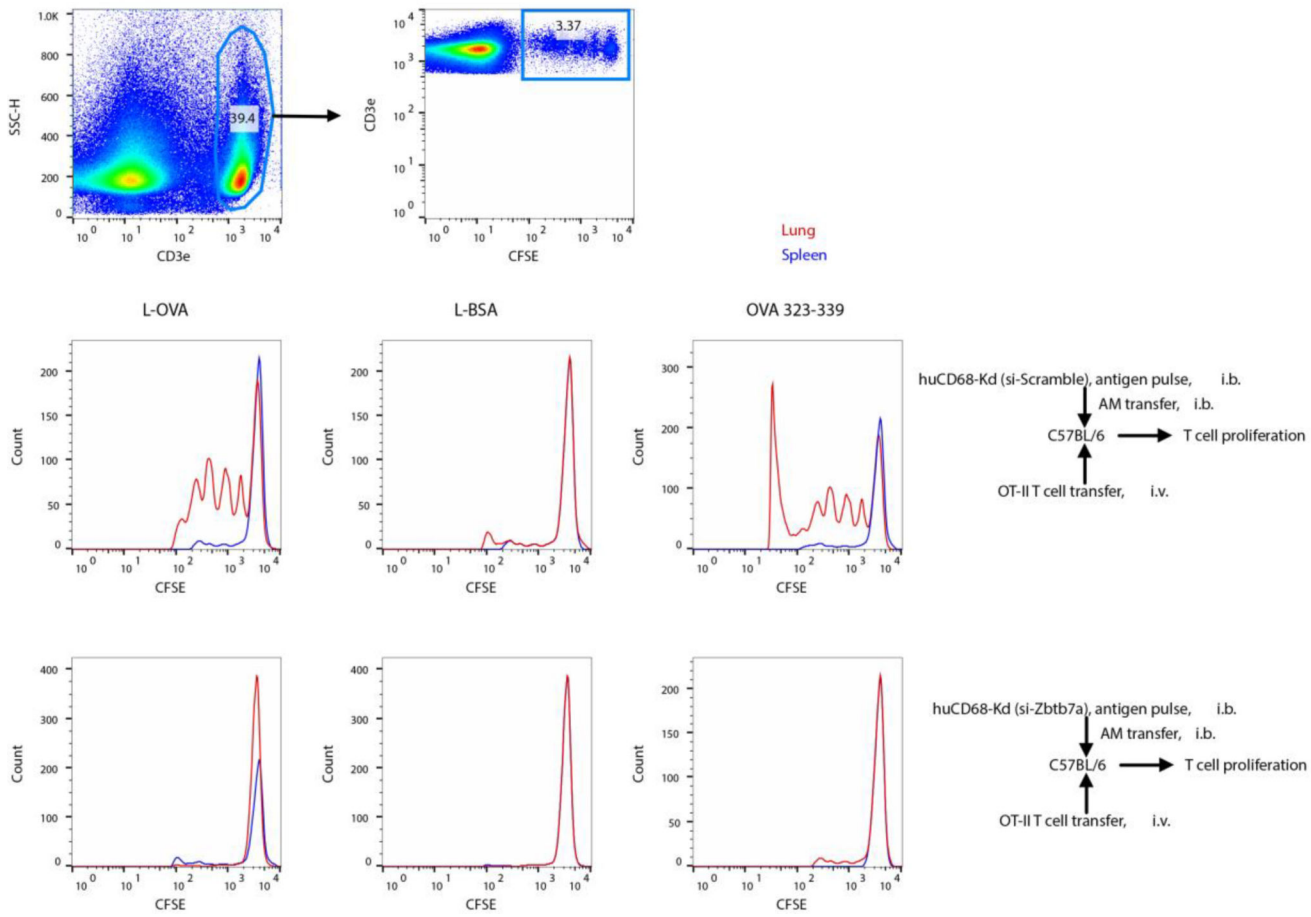

Fig. 8. Zbtb7a deficiency in AMs impairs antigen presentation

Adoptively transferred Zbtb7a-sufficient or -deficient huCD68-K^d Tg AMs in Fig. 6 were antigen pulsed (with L-OVA or L-BSA delivering 5μg of protein, or 1μg of OVA 323–339 peptide) *in vivo* at 15 wks post transfer, harvested at 6 h post pulsing and co-transferred (1×10^5) with 5×10^6 CFSE labeled naïve OT-II TCR transgenic T cells. Proliferation of OT-II T cells in lungs and spleen were measured by CFSE dilution at 72 h by gating on CFSE+, CD3+ T cells (n=5).